UNCLASSIFICATION OF THIS PAGE

REPORT DOCUMENTATION PAGE

REPORT SECURITY CLASSIFICATION	1b RESTRICTIVE MARKINGS
AD-A231 153	3 DISTRIBUTION/AVAILABILITY OF REPORT Approved for public release, distribution unlimited
	5. MONITORING ORGANIZATION REPORT NUMBER(S) AFOSR-TR- 90 1225
NAME OF PERFORMING ORGANIZATION: eorge Washington University	6b OFFICE SYMBOL (If applicable): GWU
7a NAME OF MONITORING ORGANIZATION: Air Force Office of Scientific Research/NA	
ADDRESS (City, State, and ZIP Code): ail Stop 210, ASA Langley Research Center, ampton, VA 23665	7b ADDRESS (City, State, and ZIP Code): Bldg. 410, Bolling Air Force Base, Washington, D.C. 20332
NAME OF FUNDING/SPONSORING ORGANIZATION: FOSR	8b OFFICE SYMBOL (If applicable): NA
9. PROCUREMENT INSTRUMENT IDENTIFICATION NUMBER: AFOSR-90-0252	
ADDRESS (City, State, and ZIP Code): ldg. 410, Bolling Air Force Base, ashington, D.C. 20332	10 SOURCE OF FUNDING NUMBERS: PROGRAM ELEMENT NO. 61102F; PROJECT NO. 2302; TASK NO.; WORK UNIT ACCESSION NO

TITLE (Include Security Classification)
ffective Computational Strategy for Predicting the Response of Complex Systems

PERSONAL AUTHOR(S): Ahmed K. Noor

TYPE OF REPORT	13b. TIME COVERED	14. DATE OF REPORT (Year, Month, Day)	15. PAGE COUNT
Final	FROM 3/1/90 TO 8/31/90	October 1, 1990	60

SUPPLEMENTARY NOTATION

COSATI CODES			18 SUBJECT TERMS (Continue on reverse if necessary and identify by block number)
FIELD	GROUP	SUB-GROUP	Computational strategy, predictor-corrector, symmetry transformation, operator splitting, mixed formulation, iterative techniques

ABSTRACT (Continue on reverse if necessary and identify by block number)

n effective computational strategy is developed for generating the response of complex ystems using (small or large) perturbations from the response of a simple structure (or simpler mathematical/discrete model of the original structure). Two general approaches e developed for selecting the simpler model and establishing the relations between the iginal and simpler models. The two approaches are: decomposition or partitioning rategy, and hierarchical modeling strategy. Two effective partitioning strategies are ed. The first is based on uncoupling of load-carrying mechanisms, and the second is sed on symmetry transformations. The hierarchical modeling used is a predictor-corrector erational process based on using a simple mathematical model in the predictor phase and rrecting the response using a more accurate mathematical model.

DISTRIBUTION/AVAILABILITY OF ABSTRACT: ☒ UNCLASSIFIED/UNLIMITED ☐ SAME AS RPT. ☐ DTIC USERS	21. ABSTRACT SECURITY CLASSIFICATION: Unclassified
NAME OF RESPONSIBLE INDIVIDUAL: Spencer T. Wu	22b. TELEPHONE (Include Area Code): (202) 767-6962 — 22c OFFICE SYMBOL: AFOSR/NA

FORM 1473, 84 MAR — 83 APR edition may be used until exhausted. All other editions are obsolete

SECURITY CLASSIFICATION OF THIS PAGE

Joint Institute for Advancement of Flight Sciences

THE GEORGE WASHINGTON UNIVERSITY

Final Report

Grant No. AFOSR-90-0252

EFFECTIVE COMPUTATIONAL STRATEGY FOR PREDICTING THE RESPONSE OF COMPLEX SYSTEMS

October 1990

ABSTRACT

An effective computational strategy is developed for generating the response of complex systems using (small or large) perturbations from the response of a simple structure (or a simpler mathematical/discrete model of the original structure). Two general approaches are developed for selecting the simpler model and establishing the relations between the original and simpler models. The two approaches are: decomposition or partitioning strategy, and hierarchical modeling strategy. Two effective partitioning strategies are used. The first is based on uncoupling of load-carrying mechanisms, and the second is based on symmetry transformations. The hierarchical modeling used is a predictor-corrector iterational process based on using a simple mathematical model in the predictor phase and correcting the response using a more accurate mathematical model.

RESEARCH OBJECTIVES

The objective of the present study is to develop an effective computational method for generating the response of a complex system using *large perturbations* from that of a lower-order model associated with a simpler system (or a simpler mathematical/discrete model of the original system). As an integral part of the proposed strategy an attempt will be made to unify and realize the full potential of a number of multilevel computational strategies, some of which were developed by the principal investigator and his colleagues. The multilevel strategies include *reduction methods, hybrid modeling/analysis techniques*, and *partitioning methods. Reduction methods* are techniques for substantially reducing the number of degrees of freedom of the initial discretization, and have been successfully applied to a number of vibration and nonlinear structural and thermal problems. *Hybrid modeling/analysis techniques* can achieve significant reductions in the analysis time by incorporating the known physical behavior into the computational model of the system and by using different analysis methods and/or models in predicting the different response characteristics of the engineering systems. *Partitioning methods* are based on breaking the large (and/or complex) problem into a number of smaller (and/or simpler) subproblems. The solution of the original problem is generated using information provided by the individual subproblems.

The proposed strategy is believed to combine the following three major characteristics:

1) gives physical insight about the response

2) helps in assessing the adequacy of the computational model; and

3) is highly efficient.

The strategy will first be applied to: a) the *nonlinear postbuckling problem of composite structures*; b) *reanalysis of large structures in the presence of geometric nonlinearities*; then c) *coupled field problems*. The postbuckling response of the highly anisotropic composite structure is generated using large perturbations from the response of a simpler structure. The three key elements of the strategy to be exploited in the first two applications are: 1) mixed (or primitive variable) formulation, with the fundamental unknowns consisting of both stress and displacement parameters; 2) operator splitting, or additive decomposition of the different arrays in the equations of the given structure to the corresponding arrays of the simpler, or previously-analyzed, structure plus correction terms; and c) application of a reduction method and/or a stable iterative method for the efficient generation of the equations of the given structure.

RESEARCH ACCOMPLISHMENTS

During the period March 1, 1990 to August 31, 1990, two tasks have been performed. The first is the development of an improved partitioning strategy for large-scale structural problems. The second is the development of a predictor-corrector approach for generating the steady-state thermal response of multilayered composite plates and shells. The two tasks are described subsequently.

Improved Partitioning Strategy for Large-Scale Problems

The governing equations for the discrete model of the original structure can be written in the following compact form:

$$[K]\{Z\} = \{Q\} \qquad (1)$$

where $\{Z\}$ is the vector of stress parameters and generalized displacements; $[K]$ is the global structure matrix which includes the flexibility and strain-displacement matrices; and $\{Q\}$ is the global right-hand-side vector.

In the decomposition strategy the vector of fundamental unknowns $\{Z\}$ is partitioned into

smaller subvectors. The governing discrete equations, Eqs. 1, are partitioned accordingly. The simpler model is associated wih the uncoupled equations in the partitioned variables. For the case of two partitions, the process can be described by embedding Eqs. 1 in a single-parameter family of equations as follows:

$$\left(\begin{bmatrix} K_{11} & \cdot \\ \cdot & K_{22} \end{bmatrix} + \lambda \begin{bmatrix} \cdot & K_{12} \\ K_{21} & \cdot \end{bmatrix}\right)\begin{Bmatrix} Z_1 \\ Z_2 \end{Bmatrix} = \begin{Bmatrix} Q_1 \\ Q_2 \end{Bmatrix} \tag{2}$$

where $\{Z_1\}$, $\{Z_2\}$ and $\{Q_1\}$, $\{Q_2\}$ are the partitions of the original vectors $\{Z\}$ and $\{Q\}$; λ is a tracing parameter which identifies all the correction terms needed in going from the simpler model to the discrete model of the original structure; and a dot ($\cdot$) refers to a zero submatrix. The simpler model corresponds to λ=0 (uncoupled equations in $\{Z_1\}$ and $\{Z_2\}$), and the discrete model of the original structure corresponds to λ=1 (fully coupled equations). The solution corresponding to λ=1 is generated from the corresponding solution at λ=0 using an iterative process such as the Preconditioned Conjugate Gradient (PCG). Note that the correction vectors of the iterative process, provide a direct measure of the sensitivity of the response quantities to the coupling terms (viz., the terms associated with the tracing parameter λ in Eq. 2).

The vectors $\{Z_1\}$ and $\{Z_2\}$ are chosen to be the symmetric and antisymmetric components of the response vector (each is approximately half the size of the original vector, $\{Z\}$). The simpler model (λ=0) corresponds to a symmetrized structure in which the symmetric and antisymmetric components of the response vector are uncoupled. This approach can be thought of as a *physical domain decomposition*. If the PCG technique is used in generating the solution at λ=1, and the preconditioning matrix is selected to be the left-hand side matrix corresponding to λ=0, then each of the correction vectors is either symmetric or antisymmetric.

The convergence of the PCG technique can be expedited by replacing Eqs. 2 by the following equivalent form of two *uncoupled* equations in $\{Z_1\}$ and $\{Z_2\}$:

$$\left(\begin{bmatrix} K_{11} & \cdot \\ \cdot & K_{22} \end{bmatrix} - \lambda \begin{bmatrix} K_{12}K_{22}^{-1}K_{21} & \cdot \\ \cdot & K_{21}K_{11}^{-1}K_{12} \end{bmatrix}\right)\begin{Bmatrix} Z_1 \\ Z_2 \end{Bmatrix} = \begin{Bmatrix} Q_1 \\ Q_2 \end{Bmatrix} - \lambda \begin{Bmatrix} K_{12}K_{22}^{-1}Q_2 \\ K_{21}K_{11}^{-1}Q_1 \end{Bmatrix} \tag{3}$$

Note that for λ=1, each diagonal block of the total left-hand-side matrix is in the form of Schur

complement which is not formed explicitly. Rather, the preconditioning matrix is selected to be the first matrix on the left-hand side (corresponding to $\lambda=0$) and the PCG technique is used in generating the solution at $\lambda=1$. The results of this research are reported in Ref. 1.

Predictor-Corrector Approach for Generating the Steady-State Thermal Response of Multilayered Plates and Cylinders

A predictor-corrector procedure has been developed for the accurate determination of the temperature and heat flux distributions in thick multilayered composite plates and shells. The procedure is based on using a linear through-the-thickness temperature distribution in the predictor phase. The functional dependence of temperature on the thickness coordinate is then calculated *a posteriori* and used in the corrector phase.

Extensive numerical results have been conducted for linear steady-state heat conduction problems, showing the effects of variation in the geometric and lamination parameters on the accuracy of the thermal response predictions of the predictor-corrector approach. Both antisymmetrically laminated anisotropic plates, and multilayered orthotropic cylinders are considered. The solutions are assumed to be periodic in the surface cordinates. For each problem the standard of comparison is taken to be the analytic three-dimensional solution based on treating each layer as a homogeneous anisotropic medium. The potential of the predictor-corrector approach for predicting the thermal response of multilayered plates and shells with complicated geometry is investigated. The results of this study are reported in Ref. 2.

PUBLICATIONS

1. Noor, A. K. and Peters, J. M., "Strategies for Large-Scale Structural Problems on High-Performance Computers," Communications in Applied Numerical Methods (to appear).
2. Noor, A. K., Steady-State Heat Conduction in Multilayered Composite Plates and Shells," Computers and Structures (to appear).

STRATEGIES FOR LARGE-SCALE STRUCTURAL PROBLEMS ON HIGH-PERFORMANCE COMPUTERS

Ahmed K. Noor and Jeanne M. Peters
Center for Computational Structures Technology
University of Virginia
NASA Langley Research Center
Hampton, VA 23665

SUMMARY

Novel computational strategies are presented for the analysis of large and complex structures. The strategies are based on generating the response of the complex structure using *large perturbations* from that of a simpler model, associated with a simpler structure (or a simpler mathematical/discrete model of the original structure). Numerical examples are presented to demonstrate the effectiveness of the strategies developed.

STEADY-STATE HEAT CONDUCTION IN MULTILAYERED COMPOSITE PLATES AND SHELLS

Ahmed K. Noor and W. Scott Burton
Center for Computational Structures Technology
NASA Langley Research Center
Hampton, VA 23665

ABSTRACT

A study is made of a predictor-corrector procedure for the accurate determination of the temperature and heat flux distributions in thick multilayered composite plates and shells. A linear through-the-thickness temperature distribution is used in the predictor phase. The functional dependence of temperature on the thickness coordinate is then calculated *a posteriori* and used in the corrector phase.

Extensive numerical results are presented, for linear steady-state heat conduction problems, showing the effects of variation in the geometric and lamination parameters on the accuracy of the thermal response predictions of the predictor-corrector approach. Both antisymmetrically laminated anisotropic plates, and multilayered orthotropic cylinders are considered. The solutions are assumed to be periodic in the surface coordinates. For each problem the standard of comparison is taken to be the analytic three-dimensional solution based on treating each layer as a homogeneous anisotropic medium. The potential of the predictor-corrector approach for predicting the thermal response of multilayered plates and shells with complicated geometry is discussed.

STRATEGIES FOR LARGE-SCALE STRUCTURAL PROBLEMS ON HIGH-PERFORMANCE COMPUTERS

Ahmed K. Noor and Jeanne M. Peters
Center for Computational Structures Technology
University of Virginia
NASA Langley Research Center
Hampton, VA 23665

To be Published in

Communications in Applied Numerical Methods

October 1990

STRATEGIES FOR LARGE-SCALE STRUCTURAL PROBLEMS ON HIGH-PERFORMANCE COMPUTERS

Ahmed K. Noor and Jeanne M. Peters
Center for Computational Structures Technology
University of Virginia
NASA Langley Research Center
Hampton, VA 23665

SUMMARY

Novel computational strategies are presented for the analysis of large and complex structures. The strategies are based on generating the response of the complex structure using *large perturbations* from that of a simpler model, associated with a simpler structure (or a simpler mathematical/discrete model of the original structure). Numerical examples are presented to demonstrate the effectiveness of the strategies developed.

1. INTRODUCTION

Dynamic and nonlinear response calculations for future aerospace systems are expected to require processing rates far in excess of computers built around a single processing unit. This is because of the complexity of these systems and the high degree of sophistication of the computational models required for simulating their response (see, for example, Refs. 1 and 2). The introduction of novel forms of machine architecture has brightened the prospects for meeting future large-scale computational needs. Most of the new machines achieve high performance through vectorization and/or parallelism. These include top-of-the-range supercomputers such as CRAY-3, CRAY Y-MP, as well as computing systems based on readily available and inexpensive basic units such as the hypercubes, the Connection Machine, and the transputer networks. The characteristics of several new machines are summarized in Refs. 3, 4, 5 and 6. Much work has been devoted to the development of efficient vector and parallel numerical algorithms for performing matrix operations, solution of algebraic equations, and extraction of eigenvalues (see, for example, Refs. 7, 8 and 9). Also, a number of special strategies have been proposed for increasing the degree of parallelism and/or vectorization in finite element computations. Most of

the special strategies can be thought of as applications of *multilevel computational processes*, and include reduction methods, hybrid modeling/analysis techniques, and partitioning methods. *Reduction methods* are techniques for reducing the number of degrees of freedom of the initial discretization and have been successfully applied to a number of vibration and nonlinear problems of structures (see, for example, Refs. 10-13). *Hybrid modeling/analysis techniques* can achieve significant reductions in the analysis time by incorporating the known physical behavior into the computational model of the structure and by using different analysis methods and/or models in predicting the different response characteristics of the structure (see, for example, Refs. 14 and 15). *Partitioning methods* are based on the intuitively obvious and well-established practice of breaking the large (and/or complex) problem into a number of smaller (and/or simpler) subproblems. The solution of the original problem is generated using information provided by the individual subproblems (see, for example, Ref. 16). The two key advantages of partitioning techniques are computational efficiency and modular implementation.

The present study is an attempt to unify and realize the full potential of a number of multilevel computational strategies for solution of large-scale structural problems. Specifically, the objective of the present paper is to report the progress made in developing computational strategies which, in addition to being efficient on high-performance computers, combine the following two major characteristics:

1) give physical insight about the response; and

2) help in assessing the adequacy of the computational model.

2. BASIC IDEA AND KEY ELEMENTS OF THE PROPOSED STRATEGIES

The strategies developed are based on generating the response of a large and complex structure using *large perturbations* from that of a simpler model associated with a simpler structure (or a simpler mathematical/discrete model of the original structure). The key elements of the proposed strategies are: 1) mixed (primitive variable) formulation with the fundamental unknowns consisting of stress parameters, generalized displacements and, for dynamic problems, velocity components; 2) operator splitting or restructuring of the discrete equations of the origi-

nal (complex) structure to delineate the contributions of the simpler model and the correction terms; and 3) stable iterative process for the efficient generation of the response of the complex structure starting from that of the simpler structure. Although in some applications the strategies can be used in conjunction with the single-field displacement formulation, there are several applications in which the use of the mixed formulation is essential.

2.1 Governing Equations

The governing equations for the discrete model of the original structure can be written in the following compact form:

$$[K]\{Z\} = \{Q\} \tag{1}$$

where $\{Z\}$ is the vector of stress parameters and generalized displacements; $[K]$ is the global structure matrix which includes the flexibility and strain-displacement matrices; and $\{Q\}$ is the global right-hand-side vector.

2.2 Relations Between the Original and Simpler Models

The crux of the proposed strategies is the proper selection of the simpler structure and/or the simpler model. For a given complex structure, a multitude of choices of the simpler structure can be made. The best choice is that which exploits the characteristics of the high-performance computers and satisfies, to the greatest extent possible, the two major characteristics listed in the preceding section. For each choice, the relations between the simpler model and the original structure can be established, and an efficient computational procedure can be developed for generating the response of the original structure using *large perturbations* from that of the simpler model. Two general approaches are described subsequently for selecting the simpler model and establishing the relations between the original and simpler models. The two approaches are: *decomposition or partitioning strategy*, and *hierarchical modeling strategy*. For simplicity, the two approaches are described with reference to their application to linear stress analysis problems. However, they are equally applicable to nonlinear and dynamic problems.

3. DECOMPOSITION OR PARTITIONING STRATEGY

In the decomposition strategy the vector of fundamental unknowns $\{Z\}$ is partitioned into smaller subvectors. The governing discrete equations, Eqs. 1, are partitioned accordingly. The

simpler model is associated wih the uncoupled equations in the partitioned variables. For the case of two partitions, the process can be described by embedding Eqs. 1 in a single-parameter family of equations as follows:

$$\left(\begin{bmatrix} K_{11} & \cdot \\ \cdot & K_{22} \end{bmatrix} + \lambda \begin{bmatrix} \cdot & K_{12} \\ K_{21} & \cdot \end{bmatrix}\right)\begin{Bmatrix} Z_1 \\ Z_2 \end{Bmatrix} = \begin{Bmatrix} Q_1 \\ Q_2 \end{Bmatrix} \tag{2}$$

where $\{Z_1\}$, $\{Z_2\}$ and $\{Q_1\}$, $\{Q_2\}$ are the partitions of the original vectors $\{Z\}$ and $\{Q\}$; λ is a tracing parameter which identifies all the correction terms needed in going from the simpler model to the discrete model of the original structure; and a dot ($\cdot$) refers to a zero submatrix. The simpler model corresponds to λ=0 (uncoupled equations in $\{Z_1\}$ and $\{Z_2\}$), and the discrete model of the original structure corresponds to λ=1 (fully coupled equations). The solution corresponding to λ=1 is generated from the correspondi· · solution at λ=0 using an iterative process such as the Preconditioned Conjugate Gradient (PCG). Note that the correction vectors of the iterative process, provide a direct measure of the sensitivity of the response quantities to the coupling terms (viz., the terms associated with the tracing parameter λ in Eq. 2). Among the effective partitioning strategies developed in the present study are the following two:

a) *Uncoupling of Load-Carrying Mechanisms.* For example, if the original structure is associated with a two-dimensional shell structure, the simpler structure can be associated with the corresponding plate structure in which the membrane and bending load-carrying mechanisms are uncoupled.

b) *Symmetry Transformations.* This is accomplished by selecting $\{Z_1\}$ and $\{Z_2\}$ to represent the symmetric and antisymmetric components of the response vector (each is approximately half the size of the original vector, $\{Z\}$). The simpler model (λ=0) corresponds to a symmetrized structure in which the symmetric and antisymmetric components of the response vector are uncoupled. This approach can be thought of as a *physical domain decomposition.* If the PCG technique is used in generating the solution at λ=1, and the preconditioning matrix is selected to be the left-hand side matrix corresponding to λ=0, then each of the correction vectors is either symmetric or antisymmetric. The details of the symmetry transformations are described in Refs. 17, 18 and 20.

4. COMMENTS ON THE DECOMPOSITION STRATEGY

The following comments regarding the decomposition strategy are in order:

1. The convergence of the PCG technique can be expedited by replacing Eqs. 2 by the following equivalent form of two *uncoupled* equations in $\{Z_1\}$ and $\{Z_2\}$:

$$\left(\begin{bmatrix} K_{11} & \cdot \\ \cdot & K_{22} \end{bmatrix} - \lambda \begin{bmatrix} K_{12} K_{22}^{-1} K_{21} & \cdot \\ \cdot & K_{21} K_{11}^{-1} K_{12} \end{bmatrix}\right) \begin{Bmatrix} Z_1 \\ Z_2 \end{Bmatrix} = \begin{Bmatrix} Q_1 \\ Q_2 \end{Bmatrix} - \lambda \begin{Bmatrix} K_{12} K_{22}^{-1} Q_2 \\ K_{21} K_{11}^{-1} Q_1 \end{Bmatrix} \tag{3}$$

Eqs. 3 are obtained from Eqs. 2 by eliminating $\{Z_2\}$ from the first equation and $\{Z_1\}$ from the second equation. Note that for λ=1, each diagonal block of the total left-hand-side matrix is in the form of Schur complement which is not formed explicitly. Rather, the preconditioning matrix is selected to be the first matrix on the left-hand side (corresponding to λ=0) and the PCG technique is used in generating the solution at λ=1. The technique is outlined in Appendix A.

2. Equations 3 can be thought of as the governing finite element equations of an *equivalent structure whose response under the modified loads (given by the total right-hand-side vector), is identical to the response of the actual structure when subjected to the given loads.* The equivalent structure has uncoupled load-carrying mechanisms (or uncoupled symmetric/ antisymmetric response vectors).

3. The decomposition process can be repeated to effect further reduction in the size of the partitions of the original vectors and matrices. However, as the number of partitions increases, the coupling between them increases, and therefore, the number of iterations in the PCG technique increases. Consequently, the proposed strategy may not be effective on multiprocessor computers with fine granularity and small local memories (e.g., the hypercubes and the Connection Machine of Thinking Machines, Inc.).

5. HIERARCHICAL MODELING STRATEGY

The simpler model is selected as one with considerably fewer degrees of freedom than those of the discrete model of the original structure. The governing equations of the simpler model can be written in an analogous form to those of the original structure, as follows:

$$[k]\{z\} = \{q\} \tag{4}$$

The response vectors of the original and simpler models are related through the interpolation operator $[\Gamma]$ as follows:

$$\{Z\} = [\Gamma]\{z\} \tag{5}$$

where $[\Gamma]$ is a rectangular transformation matrix (*interpolation operator*).

Based on Eqs. 4, the relations between $[k]$, $[K]$ and $\{q\}$, $[Q]$ are given by:

$$[k] = [\Gamma]^t[K][\Gamma] \tag{6}$$

$$\{q\} = [\Gamma]^t\{Q\} \tag{7}$$

where superscript t denotes transposition, and $[\Gamma]^t$ is referred to as the *restriction operator*.

Among the possible choices of the simpler model in this category are the following two:

a) *Discrete model, based on the same mathematical model and the same discretization procedure used for the original structure*, but with considerably fewer degrees of freedom. The resulting numerical process is similar to the classical multigrid technique.

b) *Discrete model, based on a mathematical model of lower dimensionality than that used for the original structure.* For example, if the original structure is modeled using a two-dimensional plate or shell theory, the simpler model can be associated with a one-dimensional thin-walled beam theory (with the effects of flexural-torsional coupling included). The interpolation operator, $[\Gamma]$, then reflects the basic assumptions made in the dimensionality reduction (i.e., in going from a two-dimensional shell/plate theory to a one-dimensional thin-walled beam theory; namely, the projection of each cross-section on a plane normal to the initial centroidal axes does not distort during deformation). This approach can, therefore, be thought of as a *physical multigrid method.*

6. NUMERICAL STUDIES

To assess the effectiveness of the foregoing strategies, a number of linear and nonlinear stress analysis, free vibration, buckling and dynamic problems of complex structures have been solved by these strategies. For each problem the solutions obtained by the foregoing strategies were compared with those obtained by the direct analysis of the original (complex) structure.

Some of these applications are reported in Refs. 17-20. Two applications of the decomposition strategies are presented herein: 1) linear stress analysis of cantilevered composite shallow shell with unsymmetrical lamination in the thickness direction; 2) nonlinear dynamic problem of laminated anisotropic panel with an off-center circular cutout. The two applications are discussed subsequently.

Both structures were modeled by using mixed finite element models with the stress resultants allowed to be discontinuous at interelement boundaries. A 12×12 grid was used for the first structure and a 192-element-grid was used for the second structure. Biquadratic shape functions were used in approximating each of the generalized displacements, and bilinear shape functions were used for approximating each of the stress resultants. The characteristics of the finite element model are given in Ref. 21.

6.1 Linear Stress Analysis of Cantilevered Composite Shallow Shell

As an application of the strategies based on uncoupling of the load-carrying mechanisms and symmetry transformations, consider the graphite-epoxy composite shallow shell with trapezoidal planform shown in Fig. 1. The shell is subjected to uniform normal loading and has nonzero curvatures k_1 and k_2 and an unsymmetric lamination in the thickness direction. The bending and membrane load-carrying mechanisms of the structure are, therefore, coupled. Also, because of the unsymmetry of the structure, the response does not exhibit any symmetry. The two decomposition strategies outlined in section 3 were applied. The number of stress and displacement degrees of freedom in each partition is given in Table 1.

a) Uncoupling of Load-Carrying Mechanisms. The simpler structure is selected to be the composite plate with zero curvatures and with the bending-extensional coupling neglected (corresponding to λ=0 in Eqs. 2 and 3).

Figure 2 shows the normalized contour plots for the generalized displacements in the original and simpler structures. The strong coupling between the in-plane and bending degrees of freedom is evident from this figure. An indication of the accuracy and convergence of the solutions obtained by using the PCG technique, in conjunction with both Eqs. 2 and 3, is given in Fig. 3. The standard of comparison is taken to be the direct solution of the original structure. As can be seen from Fig. 3, the normal displacement and total strain energy obtained by using the

PCG technique, in conjunction with both Eqs. 2 and 3, converge. However, the convergence is faster for Eqs. 3.

b) Symmetry Transformations. The simpler structure is selected to be a structure whose response vector exhibits mirror symmetry with respect to line cc (see Fig. 4). Solutions were obtained using the PCG technique, in conjunction with Eqs. 2 and 3. Also, for the sake of comparison the PCG technique was used in conjunction with the displacement finite element model which is equivalent to the mixed model used herein (see Ref. 21). The vectors $\{Z_1\}$ and $\{Z_2\}$ in Eqs. 2 and 3 are associated with displacement degrees of freedom only. Figure 4 shows the normalized contour plots for the displacements in the original and simpler structures. An indication of the accuracy and convergence of the solutions obtained by using the different PCG solutions is given in Fig. 5. As can be seen from Fig. 5, the displacement formulation results in much slower convergence than the mixed formulation and for both the mixed and displacement formulations, the use of Eqs. 3 results in faster convergence than that of Eqs. 2.

6.2 Nonlinear Dynamic Analysis of an Anisotropic Panel with an Off-Center Circular Cutout

As an application of the strategy based on symmetry transformations to nonlinear dynamic problems, consider the laminated anisotropic cylindrical panel with an off-center circular cutout shown in Fig. 6. The loading is assumed to be uniformly distributed and normal to the panel surface and has a step variation in time. The panel is made of graphite-epoxy material (see Fig. 6). Mixed finite element models were used for the spatial discretization, and implicit three-step method was used for the temporal integration.

A two-level iterative process (with two nested iteration loops) was used to generate the symmetric/antisymmetric components of the response vectors at each time step. The top level iteration (outer iteration loop) is the Newton-Raphson iteration, and the bottom-level iteration (inner iteration loop) is the PCG iteration. The PCG iteration was applied to Eqs. 2.

At each time step, three Newton-Raphson iterations and an average of 20 PCG iterations (per Newton-Raphson iteration) were required to obtain five significant digits of accuracy of the response quantities obtained using Eqs. 2. The details of the analysis are given in Ref. 20. Normalized contour plots for the displacement and velocity components at 3.0 msec, drawn on the undeformed middle surface of the panel, are shown in Fig. 7. The measured CP times and

processing rates on a single CPU for the different modules of the proposed strategy, are shown in Fig. 8. As can be seen from Fig. 7, the processing rates of most of the modules was over 175 MFLOPS and the processing rate for the most time-consuming module (module 4 - incorporation of boundary conditions and matrix decomposition) was 274.7 MFLOPS. Comparison of the wall-clock times obtained by the present strategy on one-, two- and four-CPUs, with those of the direct analysis of the panel (with no partitioning) are given in Table 2. As can be seen from Table 2, the use of the present strategy on a four CPU CRAY-YMP machine reduces the total analysis time by over one order of magnitude, compared with that required by the direct analysis (on a single processor). It is anticipated that the speedup ratios can be increased by further optimizing the Fortran code used in implementing the computational procedure of the partitioning strategy. The sustained processing rate would then be increased to that of the direct analysis implementation.

CONCLUDING REMARKS

Novel computational strategies are presented for the analysis of large and complex structures. The strategies are based on generating the response of the complex structure using large perturbations from that of a simpler structure (or a simpler mathematical/discrete model of the original structure). Two general approaches are described for selecting the simpler model and establishing the relations between the original and simpler models. The two approaches are: decomposition or partitioning strategy, and hierarchical modeling strategy. Two effective partitioning strategies are proposed. The first is based on uncoupling of load-carrying mechanisms, and the second is based on symmetry transformations. Numerical results are presented to demonstrate the effectiveness of the decomposition strategies.

ACKNOWLEDGMENT

The present research is supported by NASA Grant NAG-W-2169 and by Air Force Office of Scientific Research Grant AFOSR-90-0369. The numerical results were conducted on the CRAY-YMP at NASA Ames and the CRAY-XMP at Mendota Heights.

REFERENCES

1. Noor, A. K. and Atluri, S. N., "Advances and Trends in Computational Structural Mechanics," *AIAA Journal*, Vol. 25, No. 7, July 1987, pp. 977-995.
2. *The Federal High Performance Computing Program*, Office of Science and Technology Policy, Executive Office of the President, September 8, 1989.
3. McBryan, O. A., "State-of-the-Art in Highly Parallel Computer Systems," in *Parallel Computations and Their Impact on Mechanics*, A. K. Noor, ed., AMD-Vol. 86, American Society of Mechanical Engineers, New York, 1987, pp. 31-47.
4. Hwang, K., "Advanced Parallel Processing with Supercomputer Architectures," *Proceedings IEEE*, Vol. 75, No. 10, Oct. 1987, pp. 1348-1379.
5. Noor, A. K., "New Computing Systems and Their Impact on Computational Mechanics," in *State-of-the-Art Surveys in Computational Mechanics*, A. K. Noor and J. T. Oden, eds., American Society of Mechanical Engineers, New York, 1989, pp. 515-556.
6. Dongarra, J. J. and Duff, I. S., *Advanced Architecture Computers*, CS-89-90, Computer Science Department, Knoxville, TN, Nov. 1989.
7. Dongarra, J. J. and Sorensen, D. C., "Linear Algebra on High-Performance Computers," in *Parallel Computing 85*, M. Feilmeier, G. Joubert and U. Schendel, eds., Elsevier Science Publ., 1986, pp. 3-32.
8. McBryan, O. A. and Van de Velde, E. F., "Matrix and Vector Operations on Hypercube Parallel Processors," *Parallel Computations*, Vol. 5, Nos. 1 and 2, July 1987, pp. 117-125.
9. Ortega, J. M., *Introduction to Parallel and Vector Solution of Linear Systems*, Plenum Press, 1988.
10. Paz, M., "Practical Reduction of Structural Eigenproblems," *Journal of Structural Engineering*, Vol. 109, No. 11, 1983, pp. 2591-2599.
11. Wilson, E. L. and Itoh, T., "An Eigensolution Strategy for Large Systems," *Computers and Structures*, Vol. 6, 1983, pp. 259-265.
12. Noor, A. K., "On Making Large Nonlinear Problems Small," *Computer Methods in Applied Mechanics and Engineering*, Vol. 34, 1982, pp. 955-985.
13. Noor, A. K. and Peters, J. M., "Recent Advances in Reduction Methods for Instability

Analysis of Structures," *Computers and Structures*, Vol. 16, Nos. 1-4, 1983, pp. 67-80.

14. Kobayashi, A. S., "Hybrid Experimental-Numerical Stress Analysis," *Experimental Mechanics*, Vol. 23, No. 3, 1983, pp. 338-347.

15. Atluri, S. N. and Nishioka, T., "Hybrid Methods of Analysis," in *Unification of Finite Element Methods*, Kardestuncer, H., ed., North Holland, Amsterdam, 1984, pp. 65-95.

16. Park, K. C. and Felippa, C. A., "Partitioned Analysis of Coupled Systems," in *Computational Methods for Transient Analysis*, Belytschko, T. and Hughes, T. J. R., eds., North Holland, Amsterdam, 1983, pp. 157-219.

17. Noor, A. K. and Peters, J. M., "A Computational Strategy for Making Complicated Structural Problems Simple," *Computer Methods in Applied Mechanics and Engineering*, Vol. 71, No. 2, 1988, pp. 167-182.

18. Noor, A. K. and Whitworth, S. L., "Computational Strategy for Analysis of Quasi-symmetric Structures," *Journal of Engineering Mechanics Division, ASCE*, Vol. 114, No. 3, 1988, pp. 456-477.

19. Noor, A. K. and Whitworth, S. L., "Vibration Analysis of Quasi-symmetric Structures," *Finite Elements in Analysis and Design*, Vol. 3, 1987, pp. 257-276.

20. Noor, A. K. and Peters, J. M., "A New Partitioning Strategy for Efficient Nonlinear Finite Element Dynamic Analysis on Multiprocessor Computers," NASA TP-2850, January 1989.

21. Noor, A. K. and Andersen, C. M., "Mixed Models and Reduced/Selective Integration Displacement Models for Nonlinear Shell Analysis," *International Journal for Numerical Methods in Engineering*, Vol. 18, 1982, pp. 1429-1454.

APPENDIX A - PCG TECHNIQUE USED FOR THE SOLUTION OF EQS. 3

For convenience, Eqs. 3 can be written in the following compact form:

$$\left[|K|_0 - \lambda |K|_\lambda |K|_0^{-1} |K|_\lambda\right] \{Z\} = \{Q\}_0 - \lambda |K|_\lambda |K|_0^{-1} \{Q\}_0$$

where

$$[K]_o = \begin{bmatrix} K_{11} & . \\ . & K_{22} \end{bmatrix}, \quad [K]_\lambda = \begin{bmatrix} . & K_{12} \\ K_{21} & . \end{bmatrix}$$

$$\{Q\}_o = \begin{Bmatrix} Q_1 \\ Q_2 \end{Bmatrix}, \qquad \{Z\} = \begin{Bmatrix} Z_1 \\ Z_2 \end{Bmatrix}$$

The four major steps of the solution are:

Step 1 - Initialization

1. Obtain an initial estimate, $\{Z\}_o$ of $\{Z\}$ by solving the equations:

$$[K]_o \{Z\}_o = \{Q\}_o$$

Then obtain the vector $\{\bar{Z}\}_o$ using the equations:

$$[K]_o \{\bar{Z}\}_o = [K]_\lambda \{Z\}_o$$

2. Obtain the corresponding preconditioned residual, $\{y\}_o$ by solving the equations:

$$\begin{aligned} [K]_o \{y\}_o &= -[K]_\lambda (\{Z\}_o - \{\bar{Z}\}_o) \\ &= \{R\}_o \end{aligned}$$

where $\{R\}_o$ is the initial residual vector.

3. Set the initial conjugate search direction vectors $\{S\}_o = \{y\}_o$, and obtain the vector $\{\bar{S}\}_o$ by solving the equations:

$$[K]_o \{\bar{S}\}_o = [K]_\lambda \{S\}_o$$

Step 2 - Line Search and Updating of Solution and Residual

For i=0, begin the iteration loop and do the following:

4. Compute the step length α_i along the search direction:

$$\alpha_i = \frac{\{y\}_i^t \{R\}_i}{\{S\}_i^t \{[K]_o \{S\}_i - [K]_\lambda \{\bar{S}\}_i\}}$$

where superscript t denotes transposition.

5. Update the solution:

$$\{Z\}_{i+1} = \{Z\}_i + \alpha_i \{S\}_i$$

6. Obtain the vector $\{\bar{Z}\}_{i+1}$ using the equations:

$$[K]_o \{\bar{Z}\}_{i+1} = \{K\}_\lambda \{Z\}_{i+1}$$

7. Compute and update the new residual vector using the equations:

$$\{R\}_{i+1} = \{R\}_i - \alpha_i [K]_o \{S\}_i + [K]_\lambda \left(\{\bar{Z}\}_{i+1} - \{\bar{Z}\}_i\right)$$

Step 3 - Convergence Check

8. If $|R|_{i+1} \leq \varepsilon |R|_o$ where $|R|$ is the Euclidean norm of the residual vector and ε is a prescribed tolerance, then stop, otherwise continue.

Step 4 - Computation of New Search Direction Vector

9. Solve for the preconditioned residual vector $\{y\}_{i+1}$

$$[K]_o \{y\}_{i+1} = \{R\}_{i+1}$$

10. Compute the orthogonalization coefficient, β_{i+1}, using

$$\beta_{i+1} = \frac{\{y\}_{i+1}^t \{R\}_{i+1}}{\{y\}_i^t \{R\}_i}$$

11. Update the conjugate search direction vector

$$\{S\}_{i+1} = \{y\}_{i+1} + \beta_{i+1} \{S\}_i$$

12. Obtain the vector $\{\bar{S}\}_{i+1}$ using the equations

$$[K]_o \{\bar{S}\}_{i+1} = [K]_\lambda \{S\}_{i+1}$$

13. Step i by 1 and go to 4.

Table 1 - Number of degrees of freedom in each partition for the two decomposition strategies. Cantilevered composite shallow shell (see Fig. 1).

Nonzero Degrees of Freedom	Uncoupling of Load-Carrying Mechanisms*		Symmetry Transformations**	
	$\{Z_1\}$	$\{Z_2\}$	$\{Z_1\}$	$\{Z_2\}$
Stress Parameters	1728	2880	2304	2304
Generalized Displacements	1200	1800	1512	1488

*$\{Z_1\}$ is the vector of degrees of freedom associated with (N_1, N_2, N_{12}) and (u_1, u_2); and $\{Z_2\}$ is the vector of degrees of freedom associated with $(M_1, M_2, M_{12}, Q_1, Q_2)$ and (w, ϕ_1, ϕ_2)

**$\{Z_1\}$ and $\{Z_2\}$ are symmetric and antisymmetric components of the response vector.

Table 2 - Performance evaluation of the symmetry transformation strategy on the CRAY-YMP4/432 at CRAY Research, Inc., in Mendota Heights, MN. UNICOS 5.1.10 operating system, CFT 77 compiler version 4.0.0.

	Full Structure (optimized code)	Partitioned Structure (nearly optimized code)
Number of degrees of freedom	3818 displacements 6144 stresses	971 displacements 1536 stresses
Semibandwidth of equations	700	315
Wall clock time for first ten steps, (sec.)	171	58.6 (1 CPU) 29.7 (2 CPUs) 16.4 (4 CPUs)
Sustained speed on one CPU, MFLOPS	277.6	246
Speedup due to multiprocessing		1.0 (1 CPU) 1.95 (2 CPUs) 3.45 (4 CPUs)
Total speedup achieved by partitioning strategy	1.0	2.92 (1 CPU) 5.76 (2 CPUs) 10.43 (4 CPUs)

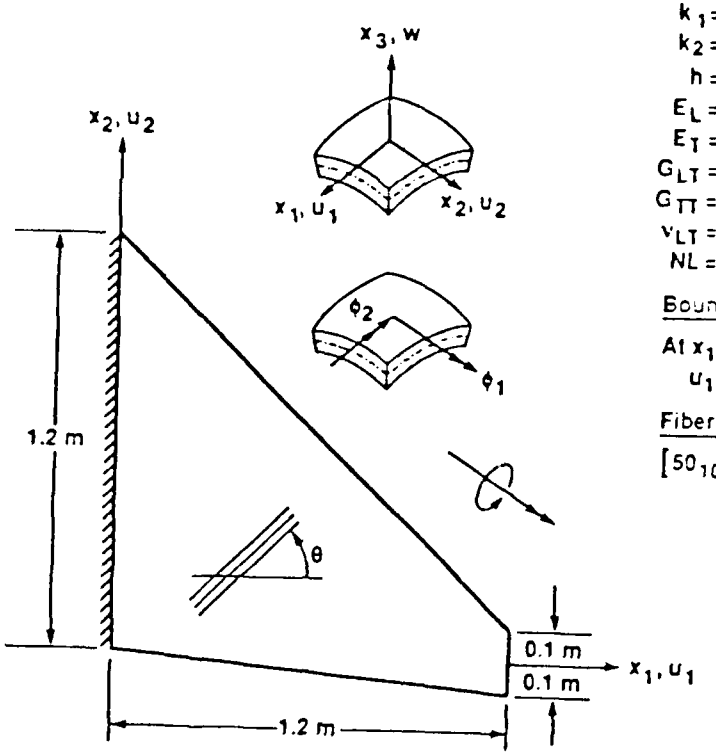

$k_1 = 0.1 \quad m^{-1}$
$k_2 = 0.08 \quad m^{-1}$
$h = 4.191 \times 10^{-3}$ m
$E_L = 134.4$ GPa
$E_T = 11.41$ GPa
$G_{LT} = 5.998$ GPa
$G_{TT} = 4.137$ GPa
$\nu_{LT} = 0.30$
$NL = 30$

Boundary conditions:

At $x_1 = 0$

$u_1 = u_2 = w = \phi_1 = \phi_2 = 0$

Fiber orientation θ:

$[50_{10}/-50_{10}/35_{10}]$

Figure 1

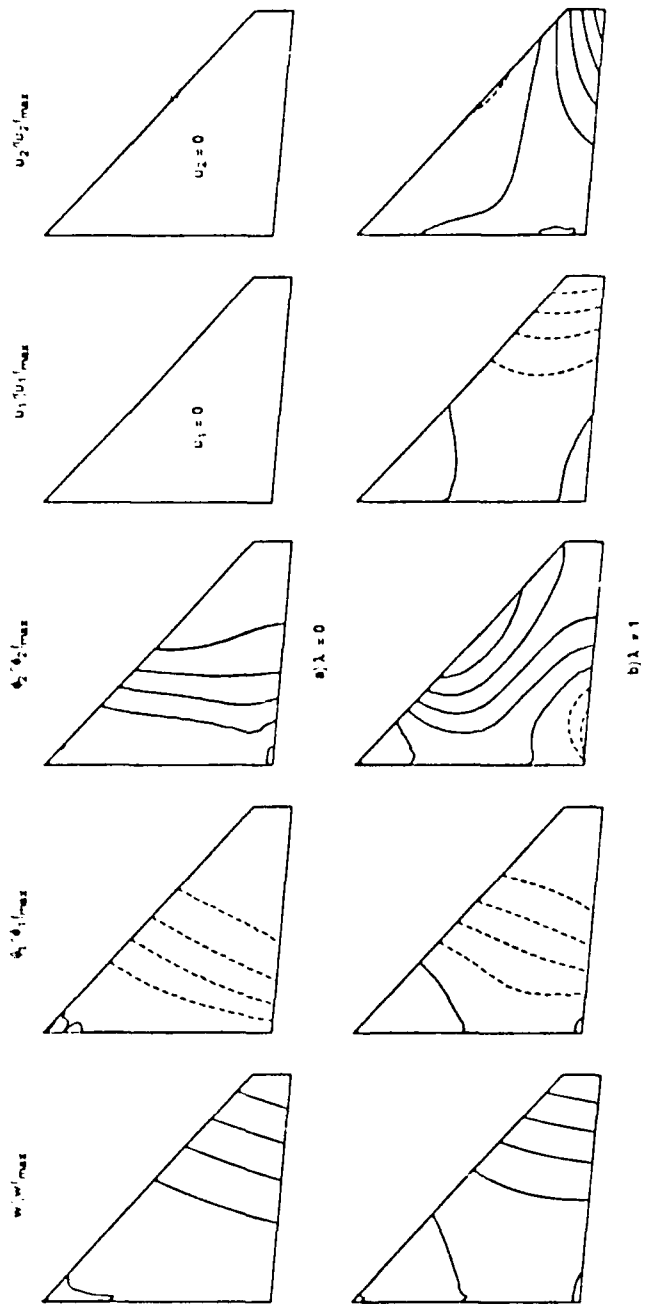

Figure 2

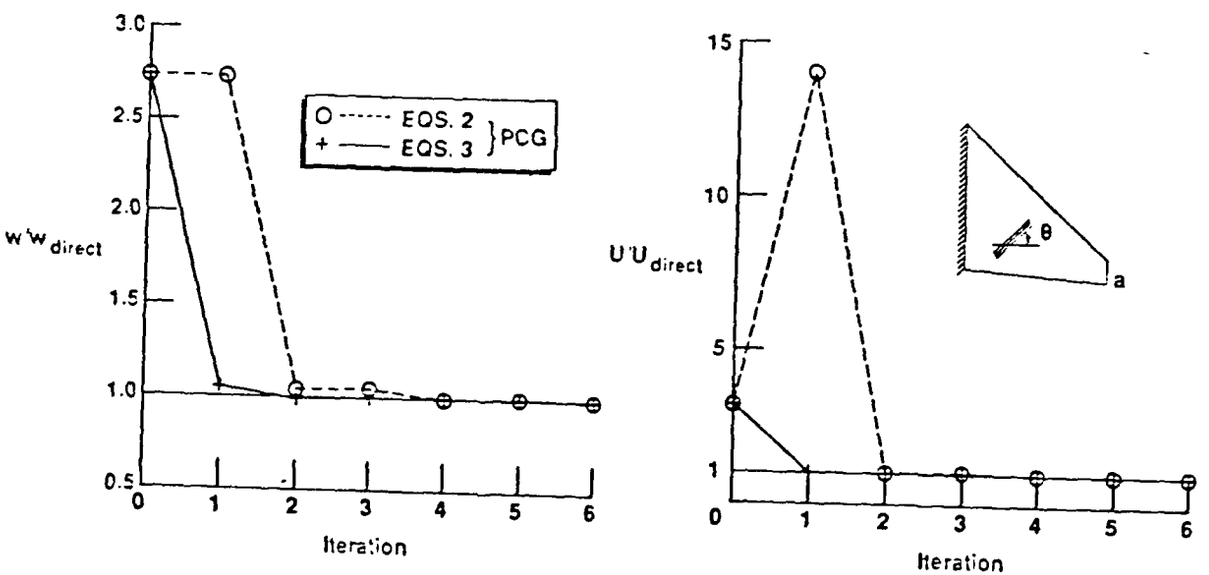
3.0
2.5
2.0
1.5
1.0
0.5
w'w direct
0
1
2
3
4
5
6
Iteration
EQS. 2
EQS. 3
PCG
15
10
5
1
U'U direct
θ
a

Figure 3

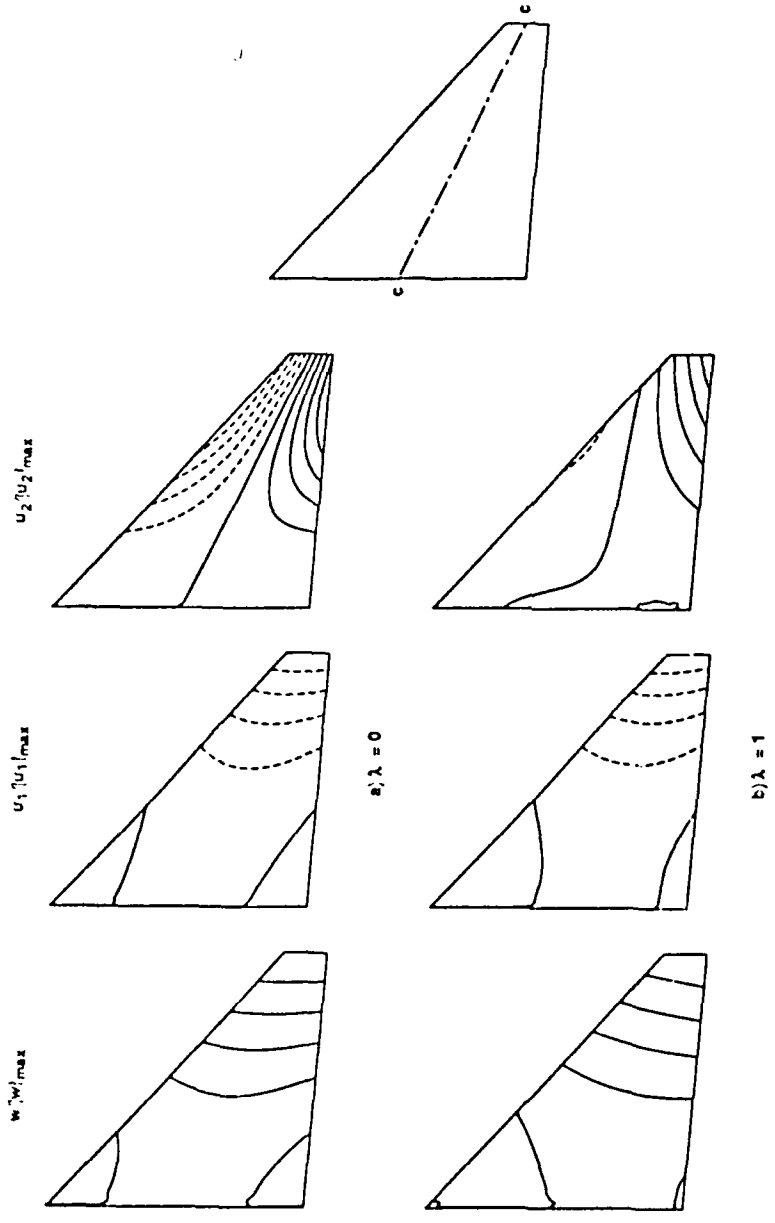

Figure 4

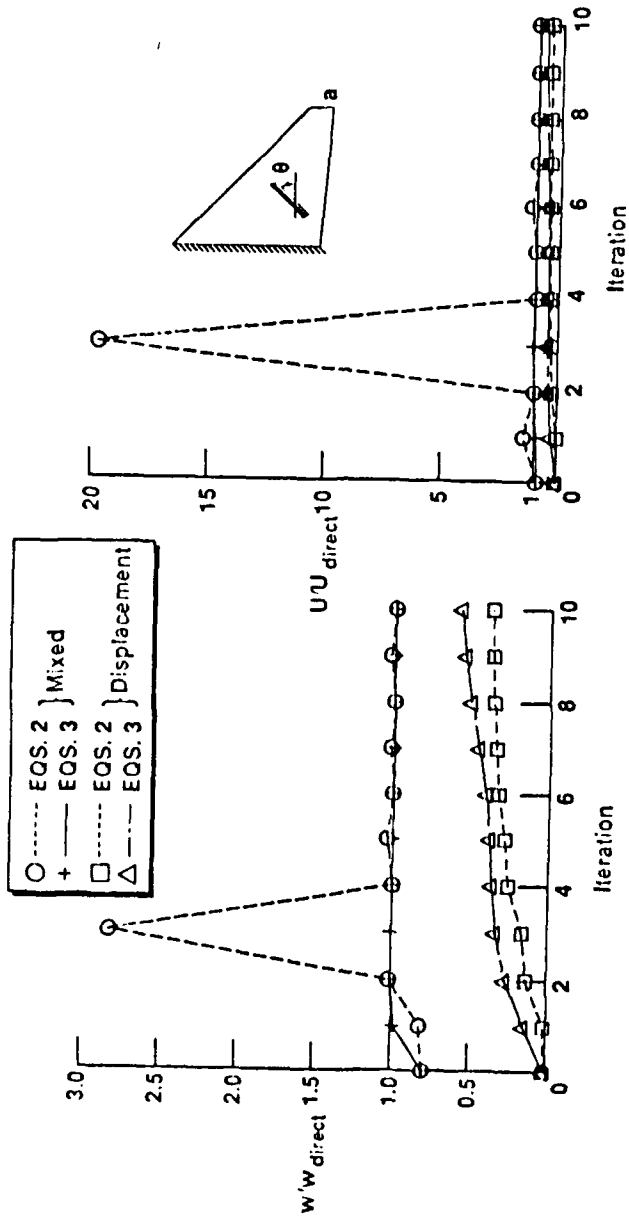
a
θ
EQS. 2 } Mixed
EQS. 3
EQS. 2 } Displacement
EQS. 3
U/U_{direct}
w/w_{direct}
Iteration
Iteration

Figure 5

STATE-OF-THE-ART SURVEYS ON COMPUTATIONAL MECHANICS

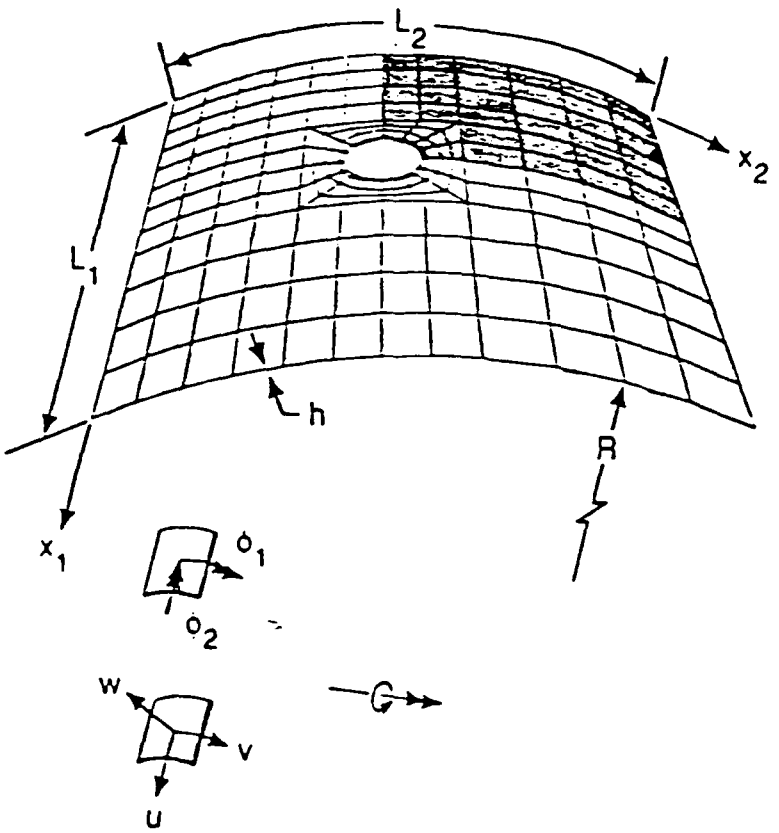

Figure 6

$L_1 = L_2 = 0.3556$ m

$R = 0.381$ m

$h = 2.276 \times 10^{-3}$ m

Hole radius = 0.0254 m

Hole center at 0.1524, 0.2032 m

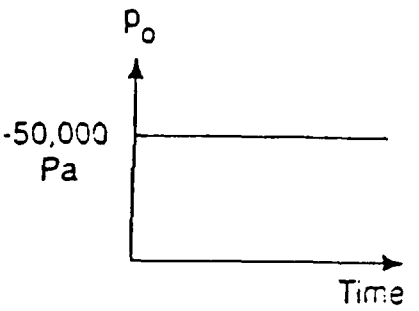

Initial conditions:

At t = 0:

$$u = v = w = \phi_1 = \phi_2 = 0$$

$$\dot{u} = \dot{v} = \dot{w} = \dot{\phi}_1 = \dot{\phi}_2 = 0$$

$E_L = 13.1 \times 10^{10}$ Pa

$E_T = 1.303 \times 10^{10}$ Pa

$G_{LT} = 6.412 \times 10^{9}$ Pa

$G_{TT} = 5.102 \times 10^{9}$ Pa

$\nu_{LT} = 0.392$

$\rho = 1522.4$ kg/m^3

Fiber orientation:

$[\pm 45/90/0_2/90/\mp 45]_S$

Boundary conditions:

At $x_1 = 0, L_1$:

$$u = v = w = \phi_1 = \phi_2 = 0$$

At $x_2 = 0, L_2$:

$$w = \phi_1 = 0$$

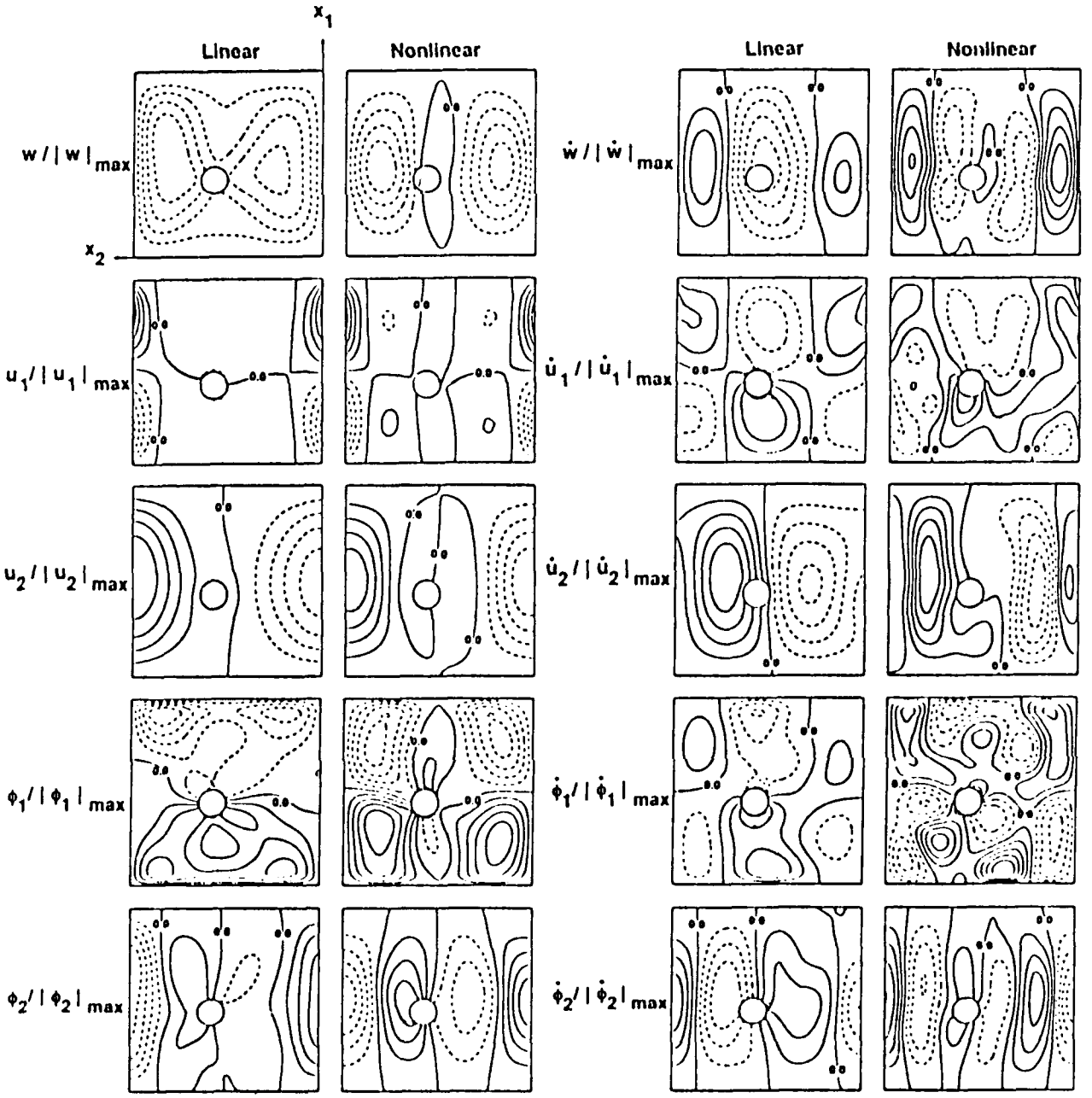

a) Generalized displacements

b) Velocity components

Figure 7

Module no.	Description
1.	Preprocessing
2.	Generation of nonlinear elemental contributions and assembling R.H.S.
3.	Eliminating stresses from L.H.S. and assembly of L.H.S.
4.	Incorporation of B.Cs. and decomposition
5.	Eliminating stresses from R.H.S.
6.	Back solve
7.	Recovery of stresses
8.	Step lengths and conjugate search directions
9.	Convergence checks

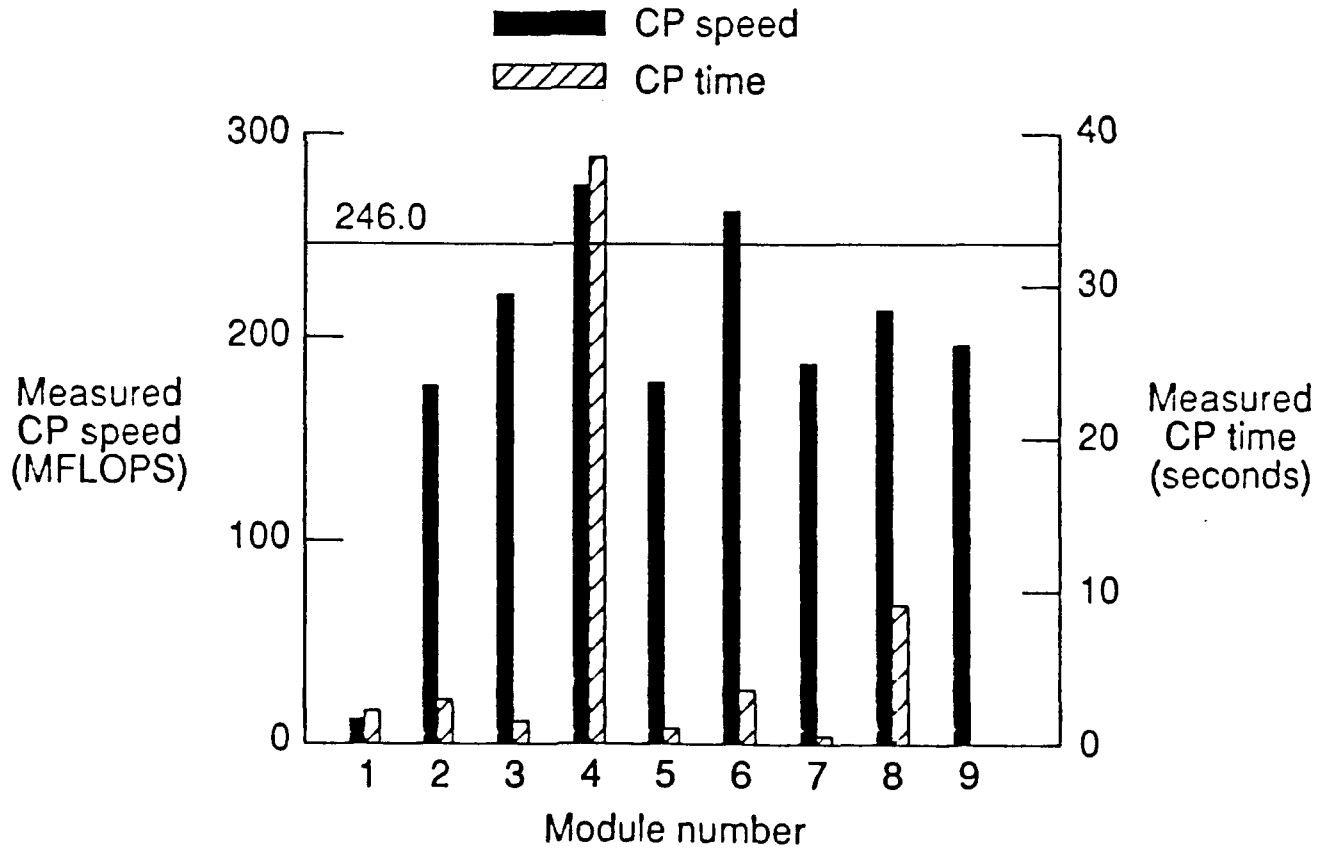

Figure 8

LIST OF FIGURES

STEADY-STATE HEAT CONDUCTION IN MULTILAYERED COMPOSITE PLATES AND SHELLS

Ahmed K. Noor and W. Scott Burton
Center for Computational Structures Technology
NASA Langley Research Center
Hampton, VA 23665

To be Published in
Computers and Structures

October 1990

STEADY-STATE HEAT CONDUCTION IN MULTILAYERED COMPOSITE PLATES AND SHELLS

Ahmed K. Noor and W. Scott Burton
Center for Computational Structures Technology
NASA Langley Research Center
Hampton, VA 23665

ABSTRACT

A study is made of a predictor-corrector procedure for the accurate determination of the temperature and heat flux distributions in thick multilayered composite plates and shells. A linear through-the-thickness temperature distribution is used in the predictor phase. The functional dependence of temperature on the thickness coordinate is then calculated *a posteriori* and used in the corrector phase.

Extensive numerical results are presented, for linear steady-state heat conduction problems, showing the effects of variation in the geometric and lamination parameters on the accuracy of the thermal response predictions of the predictor-corrector approach. Both antisymmetrically laminated anisotropic plates, and multilayered orthotropic cylinders are considered. The solutions are assumed to be periodic in the surface coordinates. For each problem the standard of comparison is taken to be the analytic three-dimensional solution based on treating each layer as a homogeneous anisotropic medium. The potential of the predictor-corrector approach for predicting the thermal response of multilayered plates and shells with complicated geometry is discussed.

NOTATION

c_q, c_T	integration constants (see Eqs. 8 and 9)
h	thickness of plate (or shell)
h_{j-1}, h_j	distance from the middle surface to the bottom and top surfaces of the jth layer, respectively
$K_{it}^{(J)}$	Integrated thermal conductivity coefficients (see Eqs. 20)
(i,t=1 to 3; J=1,2,3)	
k_{LL}, k_{TT}	thermal conductivity coefficients in the direction of fibers and normal to it,

	respectively
k_{it} (i,t=1 to 3)	thermal conductivity coefficients for a typical layer
L_1	side length of plate (or cylinder) in x_1 direction
L_2	side length of plate in x_2 direction ($2\Pi r_o$ for cylinders)
m	longitudinal wave number (in x_1 direction)
NL	number of layers of plate (or cylinder)
n	circumferential wave number
Q	internal heat generation per unit volume
$Q^{(I)}$ (I=1,2)	integrated heat generation (see Eqs. 17)
q_i (i=1 to 3)	heat flux components in the x_i coordinate directions
R_{it} (i,t=1 to 3)	thermal resistivity coefficients for a typical layer
r_o	radius of middle surface of cylinder
$S_\alpha^{(I)}$, $S_3^{(I)}$ (α,I=1,2)	integrated heat flux components (see Eqs. 17)
T	temperature
T_o, T_1	temperature functions used in first-order heat conduction theory (see Eq. 14)
x_1, x_2, x_3	orthogonal coordinate system
$\bar{\beta}$	tracing parameter identifying anisotropic terms
θ	fiber orientation angle
λ = 1	for plates
= $1 + x_3/r_o$	for cylinders
ξ_1, ξ_2, ζ	dimensionless coordinates in the x_1, x_2 and x_3 coordinate directions (see Fig. 1)
Π_t	functional defined in Eq. 5

$\Pi = \int \frac{1}{2} R_{it}\, q_i q_t \, dV$ = thermal potential of structure

Π_I	component of Π associated with the in-plane heat flux components q_1 and q_2

Π_2 component of Π associated with the transverse heat flux component q_3

Ranges of Indices (subscripts and superscripts)

I 1,2

J 1,2,3

i, t 1,2,3

j 1 to NL

α,β 1,2

INTRODUCTION

The expanded use of advanced composite materials in aerospace, automotive, shipbuilding, nuclear and other high tech industries has stimulated interest in the accurate prediction of the thermal response of laminated anisotropic plates and shells. A number of approaches have been developed for the determination of the heat transfer characteristics and thermal response of laminated anisotropic plates and shells. Some of these approaches are similar to the ones used in predicting the mechanical response of composite plates and shells and include microstructural models in which the fibers and matrix are each treated as homogeneous isotropic (or anisotropic) material (see, for example, Refs. 1, 2 and 3); and lamination theories in which the multilayered composite is replaced by an equivalent homogeneous anisotropic material and effective thermal conductivities are obtained in terms of the component conductivities (see Refs. 4, 5 and 6). Analytic, semi-analytic and finite element solutions for the heat conduction three-dimensional solids are presented in Refs. 7, 8, 9, 10, 11 and 12. A number of approaches have been proposed for the reduction of the three-dimensional heat transfer problem in laminated plates and shells to a two-dimensional problem. These include global approximation models in which the order of the governing differential equations is not dependent on the number of layers (see, for example, Ref. 13); discrete layer models (Refs. 14 and 15) in which the order of the governing differential equations depends on the number of layers, integral transform techniques (Ref. 16), and operator methods (Ref. 17).

A simple predictor-corrector procedure has been developed by the authors in Refs. 18, 19 and 20 for the accurate determination of the global as well as the detailed response characteristics

of isothermal plates and shells. The procedure is based on using the information obtained from a simple two-dimensional shear deformation theory to correct certain key elements of the computational model (in an inexpensive postprocessing mode), and hence, improve the response predictions. The present study is an adaptation of the predictor-corrector procedure to the heat transfer problem of multilayered composite plates and shells.

To sharpen the focus of the study, only linear steady-state heat conduction of composite plates and cylinders is considered. The plates are assumed to be antisymmetrically laminated with respect to the middle plane, and the cylinders are constructed of orthotropic layers. For both the plates and cylinders, the thermal response quantities are assumed to be periodic in the surface coordinates.

2. MATHEMATICAL FORMULATION

Figure 1 shows the geometric characteristics of multilayered plates and cylinders as follows: L_1 = the length of the plate (or cylinder) in the x_1 direction; h = total thickness of the plate (or cylinder); r_o = the radius of the middle surface of the cylinder; and L_2 = the length of the plate in the x_2 direction ($2\pi r_o$ for the cylinder). The dimensionless coordinates ξ_1, ξ_2, ζ are introduced, where

$$\xi_1 = \frac{x_1}{L_1} \tag{1}$$

$$\xi_2 = \frac{x_2}{\lambda L_2} \tag{2}$$

and $$\zeta = \frac{x_3}{h} \tag{3}$$

where λ=1 for plates and $1 + \frac{x_3}{r_o}$ for cylinders; and $x_3 = r - r_o$ for cylinders.

2.1 Basic Assumptions

The computational models are based on the following assumptions:

1. Each layer is considered as a homogeneous anisotropic material with the effective thermal characteristics obtained using micromechanics equations (see, for example, Refs. 5 and

6).

2. Heat transfer coefficients and thermal characteristics of all layers are independent of temperature.

3. Perfect thermal contact exists between layers (i.e., the temperature and the normal flux component are continuous at layer interfaces).

4. No heat flux is generated at the internal surfaces.

5. The thermal response is governed by two sets of equations, namely, the heat flow balance equation and the generalized Fourier's law of heat conduction. These equations are given subsequently for multilayered anisotropic plates and cylinders.

2.2 Governing Equations for Individual Layers

The governing three-dimensional equations for each layer of the plate (or shell) can be written in the following form (see, for example, Refs. 21 and 22):

a) Heat Flow Balance

$$\partial_1 q_1 + \partial_2 q_2 + \frac{1}{\lambda}\,\partial_3\,(\lambda\, q_3) - Q = 0 \tag{4}$$

and

b) Generalized Fourier's Law

$$\begin{Bmatrix} q_1 \\ q_2 \\ q_3 \end{Bmatrix} = -\begin{bmatrix} k_{11} & \bar{\beta}\,k_{12} & \bar{\beta}\,k_{13} \\ & k_{22} & \bar{\beta}\,k_{23} \\ \text{symm} & & k_{33} \end{bmatrix} \begin{Bmatrix} \partial_1 T \\ \partial_2 T \\ \partial_3 T \end{Bmatrix} \tag{5}$$

or, the inverse relations

$$\begin{Bmatrix} \partial_1 T \\ \partial_2 T \\ \partial_3 T \end{Bmatrix} = -\begin{bmatrix} R_{11} & \bar{\beta}R_{12} & \bar{\beta}R_{13} \\ & R_{22} & \bar{\beta}R_{23} \\ \text{symm} & & R_{33} \end{bmatrix} \begin{Bmatrix} q_1 \\ q_2 \\ q_3 \end{Bmatrix} \tag{6}$$

where q_i (i=1 to 3) are the flux components in the x_i coordinate directions; T is the temperature; $k_{it}=k_{ti}$ (i,t=1 to 3) are the thermal conductivity coefficients of the material of the layer; R_{it} are the thermal resistivity coefficients; Q is the internal heat generation per unit volume; $\partial_i \equiv \partial/\partial x_i$; and $\bar{\beta}$=0 and 1 for orthotropic and anisotropic layers, respectively.

Equations 4 and 6 are the stationary conditions of the following two-field functional:

$$\Pi_t(q_i, T) = \int_V \left[q_i \, \partial_i T + \frac{1}{2} \, q_i q_t \, R_{it} + QT \right] dx_1 \, dx_2 \, dx_3 \tag{7}$$

where $\partial_i \equiv \frac{\partial}{\partial x_i}$ (i = 1 to 3), and a repeated index i or t in the same term denotes summation over its full range (1 to 3).

2.3 Reduction to a Two-Dimensional Problem

In the present study, the reduction of the three-dimensional heat conduction problem described in Eqs. 4 and 5 (or 6) to a two-dimensional problem is accomplished by assuming a linear temperature variation in the thickness coordinate; and replacing the laminated plate (or shell) by an equivalent single-layer plate (or shell). The governing equations of the resulting first-order heat conduction theory are obtained by integrating Eqs. 4 and 5 in the thickness direction. Because of the discontinuity of the thermal conductivity coefficients, the integration is performed layer-by-layer. The fundamental equations of the first-order heat conduction theory are given in the Appendix.

3. PREDICTOR-CORRECTOR PROCEDURE

3.1 Basic Idea of the Procedure

The predictor-corrector procedure used in the present study is an iterational process in which the thermal response obtained in the first (predictor) phase of the analysis is used to correct the temperature distribution and, hence, improve the response predictions. Numerical experiments have shown that only one or two iterations are needed (in the corrector phase) to obtain highly accurate response predictions. The application of the procedure to multilayered composite plates and shells is described subsequently. The superscript o refers to the predictions of the first-order heat conduction theory; and a bar (-) over a symbol refers to the thermal response quantities obtained by using three-dimensional equations.

3.2 Predictor Phase

The first-order theory outlined in the previous section is used to evaluate through-the-thickness temperature, T^o, and flux components q_1^o and q_2^o. Then the flux component q_3 by

integrating Eqs. 1 in the thickness direction as follows:

$$\bar{q}_3 = -\frac{1}{\lambda}\int_{-h/2}^{x_3} \lambda\left(\partial_1 q_1^o + \partial_2 q_2^o - Q\right) dx_3 + c_q \tag{8}$$

The temperature distribution in the thickness direction, $\bar{T}$, is obtained by integrating the third equation of Eqs. 3 as follows:

$$\bar{T} = \int_{-h/2}^{x_3} \left[\bar{\beta}\left(R_{13} q_1^o + R_{23} q_2^o\right) + R_{33}\bar{q}_3\right] dx_3 + c_T \tag{9}$$

In Eqs. 8 and 9, c_q and c_T are integration constants obtained from the conditions at the outer surfaces of the laminate.

Note that because of the discontinuity of q_1 and q_2 at layer interfaces, the integrations in Eqs. 8 and 9 are performed in a piecewise manner (layer by layer).

3.3 Corrector Phase

The calculation of the corrected thermal response of the plate (or shell) may be conveniently divided into three steps: namely, 1) generation of coordinate (basis) temperature functions; 2) computation of amplitudes of the coordinate functions, and 3) evaluation of the corrected through-the-thickness flux components using three-dimensional continuum equations. The first two steps are described subsequently.

1. *Generation of Coordinate (Basis) Temperature Functions.* The temperature $\bar{T}$ is decomposed into symmetric and antisymmetric functions of the thickness coordinate x_3. Each of the symmetric and antisymmetric functions is further subdivided into an initial and correction function. The initial functions are associated with the temperature distribution T^o, obtained in the predictor phase. The correction functions are nonlinear functions in x_3 and are associated with the difference $\bar{T}-T^o$. Since the initial functions satisfy the temperature boundary conditions at the outer surfaces of the plate (or shell), the correction functions vanish on these surfaces.

2. *Computation of the Amplitudes of the Coordinate Functions.* The resulting four symmetric/antisymmetric functions associated with the temperature are now chosen as coor-

dinate (or basis functions), and the temperature is expressed as a linear combination of the four functions, with unknown parameters (representing the amplitudes of the coordinate functions (or temperature modes). The four unknown parameters are obtained by using a direct variational procedure.

Note that further improvement can be obtained by performing additional correction steps. This is accomplished by replacing T^0, q_1^0 and q_2^0 in Eqs. 8 and 9 by the response quantities obtained in the preceding corrector step and repeating the corrector phase.

4. NUMERICAL STUDIES

To assess the accuracy and effectiveness of the predictor-corrector computational procedure, a large number of heat-conduction problems of multilayered composite plates and cylinders have been solved by these techniques. The composite plates considered in the present study are square laminates with $L_1 = L_2 = 1.0$, and have antisymmetric lamination with respect to the middle plane. The composite cylinders considered are closed circular cylinders with orthotropic layers, and with $L_1 = r_0 = 1.0$. The fibers of the different layers alternate between the circumferential and longitudinal directions, with the fibers of the top layers running in the circumferential direction. The temperature boundary conditions at the top and bottom surfaces, as well as the thermal response, are periodic in x_1 and x_2 with periods $2L_1$ and $2L_2$ for plates ($2L_1$ and L_2 for cylinders).

For both the plates and the cylinders, the x_3 coordinate is a principal material direction. Moreover, for the antisymmetrically laminated plates, the thermal conductivity coefficients for a pair of layers j^+ and j^- which are symmetrically situated with respect to the middle plane satisfy the following relations:

$$\begin{aligned} k_{ii}^{(j+)} &= k_{ii}^{(j-)} && \text{(i=1 to 3 and i is not summed)} \\ k_{\alpha 3}^{(j+)} &= k_{\alpha 3}^{(j-)} = 0 && (\alpha = 1,2) \\ k_{12}^{(j+)} &= -k_{12}^{(j-)} \end{aligned} \tag{10}$$

with similar relations for the thermal resistivity coefficients.

Equations 10 are satisfied for angle-ply antisymmetric laminates, cross-ply symmetric

laminates, and combinations of the two. In the case of symmetric or unsymmetric cross-ply laminates, $k_{12}=0$ and the matrix of thermal conductivity coefficients is diagonal. The same is true for the matrix of thermal resistivity coefficients.

The material characteristics of the individual layers are taken to be those typical of high-modulus fibrous composites, namely:

$$k_{LL}=5.0 \quad , \quad k_{TT}=0.5$$

where subscript L refers to the direction of fibers and subscript T refers to the transverse direction. For plates the symmetric and antisymmetric (in the thickness direction) components of the temperature were assumed to be of the form:

$$\hat{T}_s \sin \pi\xi_1 \quad \sin \pi\xi_2 \quad \text{and} \tag{11}$$

$$\hat{T}_a \cos \pi\xi_1 \quad \cos \pi\xi_2 \tag{12}$$

where subscripts s and a refer to the symmetric and antisymmetric components (in the thickness direction). The values of $\hat{T}_s$ and $\hat{T}_a$ at the top surface of the plate are given by $\hat{T}_s = 250$ and $\hat{T}_a = 50$. Note that the trigonometric functions used in describing the surface distributions of the symmetric and antisymmetric components of the temperature are different.

For cylinders, the temperature distribution was assumed to be of the form:

$$\begin{pmatrix} T_o \\ T_i \end{pmatrix} = \begin{pmatrix} \hat{T}_o \\ \hat{T}_i \end{pmatrix} \cos \pi \xi_1 \quad \cos 2\pi n \xi_2 \tag{13}$$

where $\hat{T}_o = 300$ and $\hat{T}_i = 200$. Subscripts o and i refer to the outer (top) and inner (bottom) surfaces of the cylinder, respectively. For each problem, the solutions obtained by the four models described in Table 1 were compared with the analytic three-dimensional continuum solutions.

Table 1 - Characteristics of the models used in the numerical studies

Model	Predictor Phase	Number of iterations in the corrector phase
1	First-order heat conduction theory	0
2	(based on assuming a linear temperature	1
2A	variation in the thickness coordinate)	2
2B		3

For plates, three parameters were varied, namely: the thickness ratio of the plate, h/L_1; the number of layers, NL; and the fiber orientation angle of the individual layers, θ. The thickness ratio was varied between 0.01 and 0.5; the number of layers was varied between 2 and 20; and θ was varied between 0° and 45°. For cylinders, three parameters were varied, namely: the thickness ratio h/r_o; the number of layers, NL; and the circumferential wave number, n. The longitudinal wave number was selected to be 1, and the length-to-radius ratio, L/r_o, was selected to be 1.0. The number of layers was varied between 2 and 20; h/r_o between 0.01 and 0.5, and n between 0 and 10.

As a step towards establishing the range of validity of the predictor-corrector procedure and the number of iterations required in the corrector phase, the thermal potential of the structure, $\Pi = \int \frac{1}{2} R_{it} q_i q_t \, dV \quad (i,t = 1 \text{ to } 3)$; was decomposed into two components: Π_1 associated with q_1 and q_2; and Π_2 associated with q_3 ($\Pi_2 = \int \frac{1}{2} R_{33} q_3 q_3 \, dV$). The total thermal potential of the structure $\Pi = \Pi_1 + \Pi_2$. The assessment of the predictor-corrector procedure included both the global thermal response characteristics, Π, Π_1 and Π_2, as well as detailed temperature and flux distributions in the thickness direction.

Typical results are given in Figs. 2, 3 and 4 for the antisymmetrically laminated plates, and in Figs. 5, 6 and 7 for the multilayered orthotropic cylinders. The effects of variation of the two parameters, h/L_1, NL for plates (and h/L_1 and n for cylinders) on the thermal potential compo-

nents Π_1 and Π_2, obtained by the three-dimensional continuum model are depicted in Fig. 2 for plates and in Fig. 5 for cylinders.

An indication of the accuracy of the thermal potential components Π_1 and Π_2, obtained by the predictor-corrector procedure, is given in Figs. 3 and 6. Figures 4 and 7 give an indication of the accuracy of the temperature and heat flux distributions in the thickness direction. In Fig. 4 both the symmetric and antisymmetric parts of the thermal response quantities (with respect to the middle plane) are shown. Note that since the symmetric and antisymmetric components of each thermal response quantity are multiplied by different trigonometric functions in x_1 and x_2, the value of the response quantity is a linear combination of the two components.

An examination of Figs. 2 to 7 reveals:

1. The ratio of the thermal potential component Π_1/Π increases rapidly with the increase in h/L_1 from 0.01 up to h/L_1=0.1 for plates (and h/L_1 from 0.01 to 0.15 for cylinders with $n \leq 2$). The decrease in Π_1/Π is associated with a sharp decrease in Π_2/Π. Further increases in h/L_1 are associated with a slow decrease in Π_1/Π and a slow increase in Π_2/Π (see Figs. 2 and 5).

2. The ratios Π_1/Π and Π_2/Π are somewhat insensitive to variations in the number of layers NL. For plates these ratios are also somewhat insensitive to the fiber orientation angle θ (results not shown).

3. For antisymmetrically laminated plates, the accuracy of the predictions of the first-order heat-conduction theory, Model 1, deteriorates rapidly as h/L_1 increases. This is true for both the global as well as the detailed thermal response characteristics. For plates with NL=10, θ=45°, h/L_1=0.1, the error in Π predicted by Model 1 was 7.4% and increased to 165% for h/L_1=0.3 (see Fig. 3).

4. The accuracy of the predictions of the first-order theory and its range of validity can be significantly improved by using one or two iterations in the corrector phase, Models 2 and 2A, even for very thick plates and shells. As an example to this, for plates with h/L_1=0.5, the error in Π was 249%. The corresponding errors after one and two iterations in the corrector phase were only 3.2% and 0.08%, respectively (see Fig. 3).

5. For orthotropic cylinders the accuracy of the predictions of Model 1 deterioriates

rapidly as the circumferential wave number, n, increases. As an example to this, for cylinders with h/r_o=0.5, NL=10, n=2, the error in Π predicted by Model 1 was 220%, and increased to 378% for n=6. The use of one and two iterations in the corrector phase (Models 2 and 2A) reduced the errors for n=6 to 9.8% and 0.64%, respectively (see Fig. 6).

6. The thickness distributions of temperature and flux components obtained by the predictor-corrector approach are highly accurate. For plates and cylinders with $h/L_1 \leq 0.5$ and $n \leq 5$, the distributions of the response quantities after two iterations (Model 2A) in the corrector phase were almost indistinguishable from the exact three-dimensional solutions (see, for example, Figs. 4 and 7).

7. Numerical experiments (not presented herein) have shown that the use of higher-order heat conduction theories for multilayered composites based on a global cubic variation, or higher-degree polynomial approximation, for the temperature through the thickness results in highly accurate temperature, as well as heat flux components q_1 and q_2. However, the transverse heat flux component q_3 obtained by these theories is not as accurate.

5. POTENTIAL OF THE PREDICTOR-CORRECTOR PROCEDURE

The predictor-corrector procedure appears to have high potential for the accurate prediction of the thermal response of multilayered composite plates and shells. The numerical studies conducted for antisymmetrically laminated anisotropic plates and simply supported orthotropic cylinders demonstrated the accuracy and effectiveness of the predictor-corrector procedure. In particular, the following two points are worth mentioning:

1. The predictor-corrector procedure can be applied, in conjunction with finite element models, to the analysis of anisotropic plates and shells with arbitrary geometry. The calculation of the heat flux component in the transverse direction, and the correction phase (including the calculation of the transverse temperature distribution) can be performed on the element level for selected elements (in the critical regions of the plate and shell models).

2. Although any of the two-dimensional heat conduction models can be used in the first (predictor) phase of the predictor-corrector procedure, the first-order theory involves fewer temperature parameters than higher-order theories.

6. CONCLUDING REMARKS

A study is made of a predictor-corrector procedure for the accurate determination of the temperature and heat flux distributions in thick multilayered composite plates and shells. A first-order heat conduction theory, based on linear through-the-thickness temperature distribution, is used in the predictor phase. The functional dependence of temperature on the thickness coordinate is then calculated *a posteriori* and used in the corrector phase.

Extensive numerical results are presented, for linear steady-state heat conduction problems, showing the effects of variation in the geometric and lamination parameters on the accuracy of the thermal response quantities obtained by the predictor-corrector approach. Both antisymmetrically laminated anisotropic plates, and multilayered orthotropic cylinders are considered. The solutions are assumed to be periodic in the surface coordinates, and for each problem the standard of comparison is taken to be the analytic three-dimensional solution based on treating each layer as a homogeneous anisotropic medium.

The numerical results clearly demonstrate the effectiveness of the predictor-corrector procedures for the accurate determination of the global as well as detailed thermal response characteristics of multilayered plates and shells. The accuracy of the response quantities obtained in the first (predictor) phase for thick laminates ($h/L_1 \geq 0.1$) may be unacceptable. However, the use of one or two iterations in the corrector phase improves the predictions substantially and results in highly accurate distributions of temperature and heat flux components through the thickness.

ACKNOWLEDGEMENT

The present research is partially supported by NASA Grant NAG-W-2169 and by Air Force Office of Scientific Research Grant AFOSR-90-0369.

REFERENCES

1. G. N. Dul'nev and Y. P. Zarichnyak, A study of generalized conductivity coefficients in heterogeneous systems. *Heat Transfer - Soviet Research* **2**(4), 89-107 (July 1970).

2. B. A. Boley, Survey of recent developments in the fields in heat conduction in solids and thermo-elasticity. *Nuc. Eng. and Design* **18**(3), 377-399 (Feb. 1972).

3. J. L. White and Knutsson, A., Theory of thermal conductivity, heat conduction and convective heat transfer in fiber filled polymer composites. *Polymer Eng. Review* **2**(1), 71-82 (1982).

4. F. K. Tsou, P. C. Chou and I. Singh, Apparent tensorial conductivity of layered composites. *AIAA Journal* **12**(12), 1693-1698 (Dec. 1974).

5. S. W. Tsai and H. T. Hahn, *Introduction to Composite Materials*. Technomic Pub. Co., Westport, CT (1980).

6. Chamis, C. C., *Simplified Composite Micromechanics Equations for Hygral, Thermal and Mechanical Properties*, NASA TM 83320 (1983).

7. M. A. Brull and J. R. Vinson, Approximate three-dimensional solutions for transient temperature distribution in shells of revolution. *Journal of the Aero/Space Sciences* 742-750 (Dec. 1958).

8. J. Padovan, Semi-analytical finite element procedure for conduction in anisotropic axisymmetric solids. *Int. Journal for Numerical Methods in Engineering* **8**, 295-310 (1974).

9. Y. P. Chang and R. C. H. Tsou, Heat conduction in an anisotropic medium homogeneous in cylindrical regions - steady state. *Journal of Heat Transfer*, ASME 132-134 (Feb. 1977).

10. G. P. Mulholland and B. P. Gupta, Heat transfer in a three-dimensional anisotropic solid of arbitrary shape. *Journal of Heat Transfer*, ASME 135-137 (Feb. 1977).

11. K. S. Surana and N. J. Orth, p-approximation axisymmetric shell elements for heat conduction in laminated composites. *Computers and Structures* **33**(5), 1251-1265 (1989).

12. K. S. Surana and G. Abusaleh, Curved shell elements for heat conduction with p-approximation in the shell thickness direction. *Computers and Structures* **34**(6), 861-880 (1990).

13. V. S. Sipetov, Accurate analysis of the behavior of laminated composite structures on the thermal and static effects. *Mekhanika Kompozitnykh Materialov* **25**(1), 142-149 (Jan./Feb. 1989) (English translation in *Mechanics of Composite Materials* **25**(1), 123-130 (1989)).

14. E. I. Grigolyuk and P. P. Chulkov, Equations of the temperature field for three-layered

shells. *Izvestia Akad. Nauk. SSR*, Tekhn. n. **6**(2) (1964) (English translation in *Mechanics of Solids* **7**(3) 89-93 (1973)).

15. I. A. Motorilovets and V. I., *Mechanics of Connected Fields in Structural Members - Vol. 1, Thermoelasticity*. Naukovâ, Dumka, Kiev (in Russian)(1987).
16. J. Padovan, Temperature distributions in anisotropic shells of revolution. *AIAA Journal* **10**(1), 60-64 (Jan. 1972).
17. S. G. Beregovoy, Ya. S. Podstrigach and Yu. A. Chernukha, Heat conduction equations for multilayer shells. *Izvestia AN SSSR, Mekhanika Tverdogo Tela* **7**(3), 105-110 (1972).
18. A. K. Noor and W. S. Burton, Assessment of Computational Models for Multilayered Anisotropic Plates. *Composite Structures* **14**, 233-265 (1990).
19. A. K. Noor and W. S. Burton, Assessment of Computational Models for Multilayered Composite Shells. *Applied Mechanics Reviews* **43**(4), 67-97 (1990).
20. A. K. Noor, W. S. Burton and J. M. Peters, Predictor-Corrector Procedure for Stress and Free Vibration Analyses of Multilayered Composite Plates and Shells. *Computer Methods in Applied Mechanics and Engineering* (to appear).
21. H. S. Carslaw and J. C. Jaeger, *Conduction of Heat in Solids*. Oxford Clarendon Press, London (1959).
22. M. N. Ozisik, *Heat Conduction - Theory and Application*. John Wiley & Sons, New York (1980).

APPENDIX - FUNDAMENTAL EQUATIONS OF THE FIRST-ORDER HEAT CONDUCTION THEORY USED IN THE PRESENT STUDY

The fundamental equations of the two-dimensional first-order heat conduction theory used in the present study are given in this appendix.

Temperature Distribution

The temperature is assumed to have a linear variation in the thickness coordinate as follows:

$$T = T_0 + x_3 T_1 \tag{14}$$

where T_0 and T_1 are functions of x_1 and x_2.

Heat Balance Equations

The two global heat balance equations can be written in terms of the integrated heat flux

components as follows:

$$\partial_\alpha S_\alpha^{(I)} - Q^{(I)} + (\lambda q_3)\big|_{x_3=h/2} - (\lambda q_3)\big|_{x_3=-h/2} = 0 \tag{15}$$

$$\partial_\alpha S_\alpha^{(2)} - S_3^{(I)} - Q^{(2)} + (x_3 \lambda q_3)\big|_{x_3=h/2} - (x_3 \lambda q_3)\big|_{x_3=-h/2} = 0 \tag{16}$$

where

$$\begin{Bmatrix} S_\alpha^{(I)} \\ S_3^{(I)} \\ Q^{(I)} \end{Bmatrix} = \sum_{j=1}^{NL} \int_{h_{j-1}}^{h_j} \begin{Bmatrix} \gamma_{(\alpha)}\, q_\alpha\, x_3^{(I-1)} \\ \lambda\, q_3 \\ \lambda\, Q\, x_3^{(I-1)} \end{Bmatrix} dx_3 \tag{17}$$

with $\gamma_{(1)} = \lambda$ and $\gamma_{(2)} = 1$, $\alpha = 1,2$ and $I = 1,2$. Note that a repeated index α in Eqs. 15 and 16 denotes summation over the range 1,2; and α is not summed in Eqs. 17.

Generalized Fourier's Law

$$S_\alpha^{(I)} = -K_{\alpha\beta}^{(I)}\, \partial_\beta T_o - K_{\alpha 3}^{(I)}\, T_1 - K_{\alpha\beta}^{(I+1)}\, \partial_\beta T_1 \tag{18}$$

$$S_3^{(I)} = -K_{\beta 3}^{(I)}\, \partial_\beta T_o - K_{33}^{(I)}\, T_1 - K_{\beta 3}^{(2)}\, \partial_\beta T_1 \tag{19}$$

where

$$K_{i\iota}^{(J)} = \sum_{j=1}^{NL} \int_{h_{j-1}}^{h_j} \nu_{(i)}\, \nu_{(\iota)}\, k_{i\iota}\, x_3^{(J-1)}\, dx_3 \tag{20}$$

with $\nu_{(1)} = \nu_{(3)} = \sqrt{\lambda}$, $\nu_{(2)} = 1/\sqrt{\lambda}$; $J = 1,2,3$; $i,\iota = 1,2,3$; and $\alpha,\beta = 1,2$. Note that a repeated index β in Eqs. 18 and 19 denotes summation over the range 1,2; and i,ι are not summed in Eqs. 20.

Governing Equations

The two governing differential equations in the temperature functions T_o and T_1 are obtained by replacing the quantities $S_\alpha^{(I)}$, $S_3^{(I)}$ in Eqs. 14 and 15 by their expressions in terms of T_o and T_1 (Eqs. 19 and 20).

Trigonometric Functions for the Temperature and Integrated Heat Flux Components

The temperature and integrated heat flux components are assumed in the present study to be periodic in both the x_1 and x_2 directions with periods of $2L_1$ and $2L_2$ for plates (and $2L_1$, L_2 for cylinders). The following products of trigonometric functions are used for the different response quantities:

Antisymmetrically laminated plates:

$$T_o = T_{o_{mn}} \sin m\pi\xi_1 \sin n\pi\xi_2 \tag{21}$$

$$\left(T_1, S_3^{(1)}\right) = \left(T_{1_{mn}}, S_{3_{mn}}^{(1)}\right) \cos m\pi\xi_1 \cos n\pi\xi_2 \tag{22}$$

$$\left(S_1^{(1)}, S_2^{(2)}\right) = \left(S_{1_{mn}}^{(1)}, S_{2_{mn}}^{(2)}\right) \cos m\pi\xi_1 \cos n\pi\xi_2 \tag{23}$$

$$\left(S_2^{(1)}, S_1^{(2)}\right) = \left(S_{2_{mn}}^{(1)}, S_{1_{mn}}^{(2)}\right) \sin m\pi\xi_1 \cos n\pi\xi_2 \tag{24}$$

Multilayered orthotropic cylinders:

$$\left(T_o, T_1, S_3^{(1)}\right) = \left(T_{o_{mn}}, T_{1_{mn}}, S_{3_{mn}}^{(1)}\right) \cos m\pi\xi_1 \cos 2\pi n\xi_2 \tag{25}$$

$$\left(S_1^{(1)}, S_1^{(2)}\right) = \left(S_{1_{mn}}^{(1)}, S_{1_{mn}}^{(2)}\right) \sin m\pi\xi_1 \cos 2\pi n\xi_2 \tag{26}$$

$$\left(S_2^{(1)}, S_2^{(2)}\right) = \left(S_{2_{mn}}^{(1)}, S_{2_{mn}}^{(2)}\right) \cos m\pi\xi_1 \sin 2\pi n\xi_2 \tag{27}$$

The governing equations can be reduced to a set of algebraic equations through the use of the trigonometric functions, Eqs. 21 to 27. Note that the trigonometric functions, Eqs. 21 to 27, provide exact solution for the governing differential equations of antisymmetrically laminated plates and multilayered orthotropic cylinders.

LIST OF FIGURES

Figure 7 - Accuracy of temperature and heat flux components obtained by predictor-corrector procedure. Multilayered composite cylinders with prescribed surface temperatures $T_o = \hat{T}_o \cos \pi\xi_1 \cos 2\pi n\xi_2$, $T_i = \hat{T}_i \cos \pi\xi_1 \cos 2\pi n\xi_2$; $\hat{T}_o = 300$, $\hat{T}_i = 200$, $L/r_o = 1.0$, $h/r_o = 0.5$, NL=10, and $n=1$.

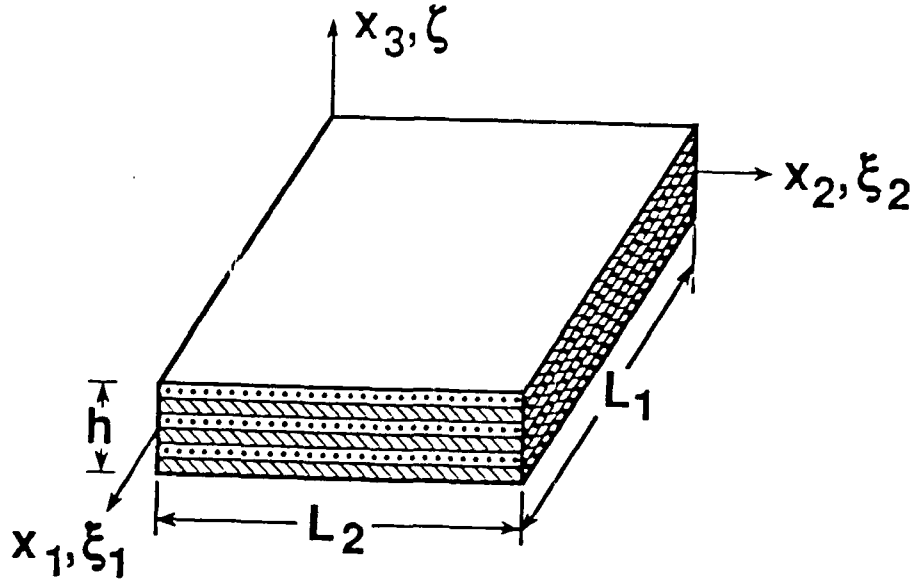
x3, ζ
x2, ξ2
h
L1
L2
x1, ξ1

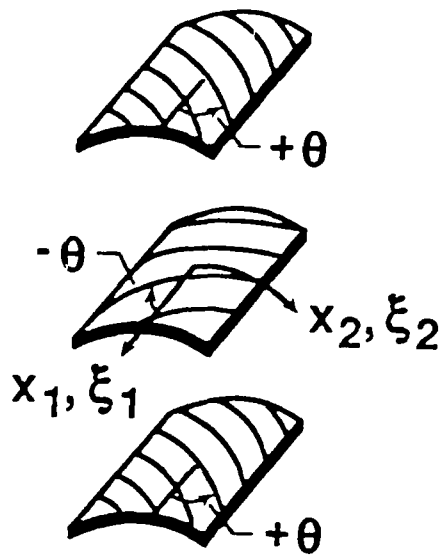
+θ
-θ
x2, ξ2
x1, ξ1
+θ

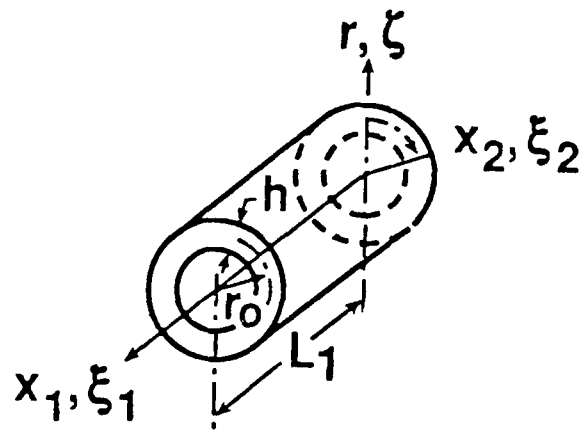
r, ζ
x2, ξ2
h
ro
L1
x1, ξ1

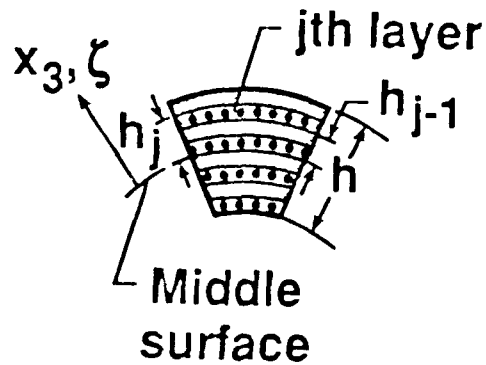
jth layer
x3, ζ
hj
hj-1
h
Middle
surface

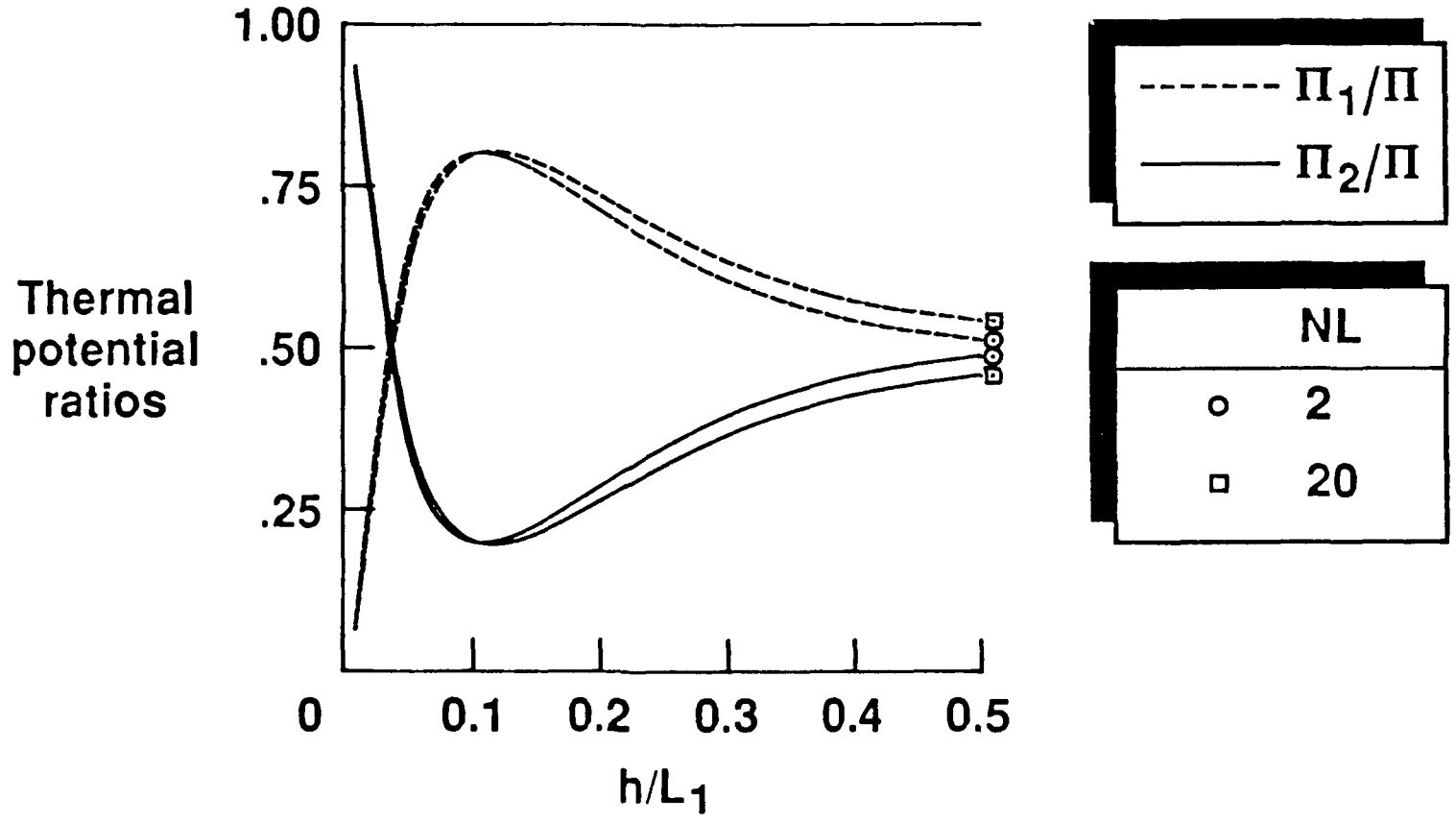
1.00
.75
.50
.25
0
0.1
0.2
0.3
0.4
0.5
Thermal potential ratios
h/L1
Π1/Π
Π2/Π
NL
2
20

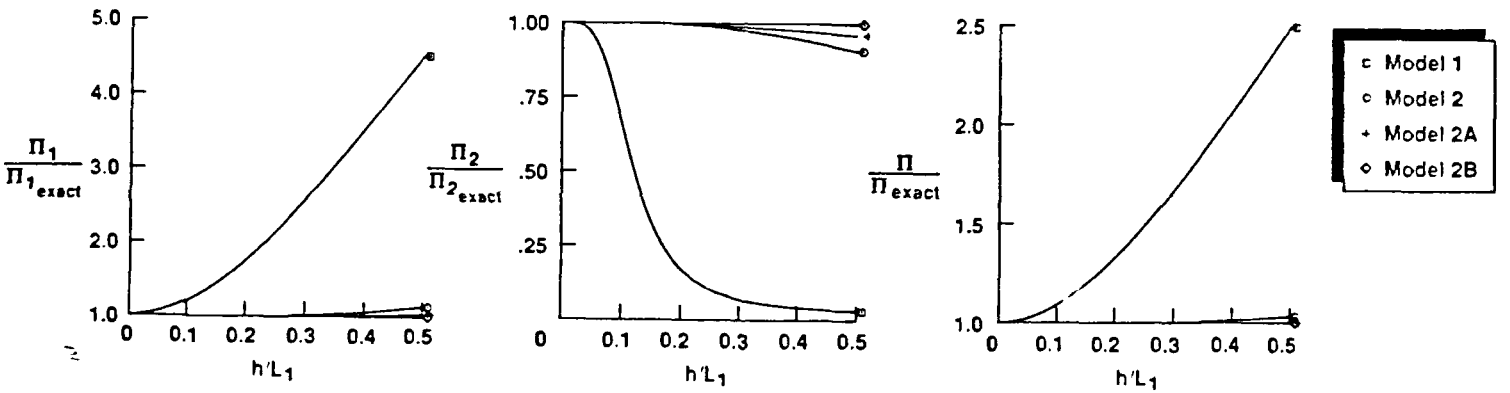
$\frac{\Pi_1}{\Pi_{1_{exact}}}$
5.0
4.0
3.0
2.0
1.0
0
0.1
0.2
0.3
0.4
0.5
h'L1
$\frac{\Pi_2}{\Pi_{2_{exact}}}$
1.00
.75
.50
.25
0
0.1
0.2
0.3
0.4
0.5
h'L1
$\frac{\Pi}{\Pi_{exact}}$
2.5
2.0
1.5
1.0
0
0.1
0.2
0.3
0.4
0.5
h'L1
Model 1
Model 2
Model 2A
Model 2B

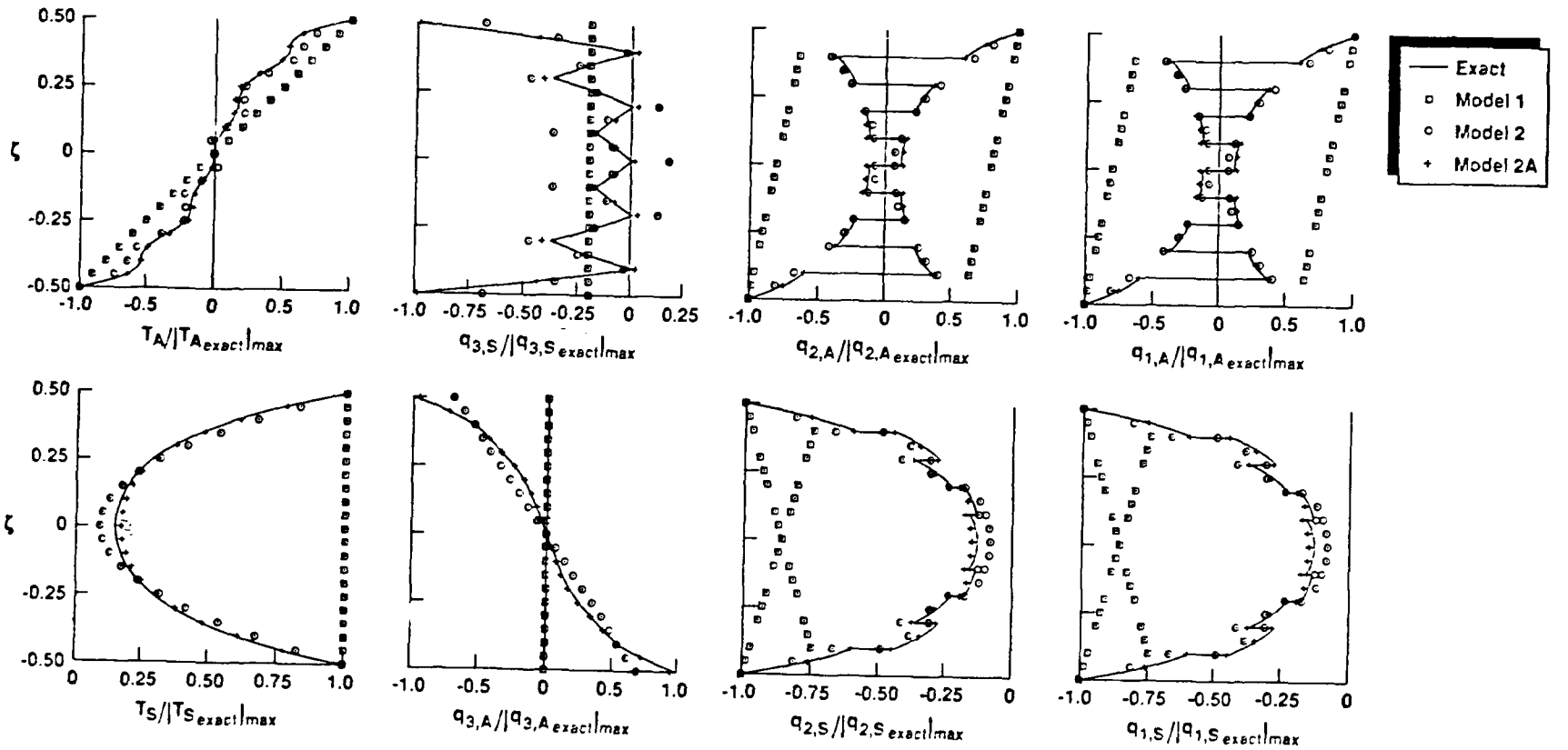
Exact
Model 1
Model 2
Model 2A
ζ
$T_A/|T_{A_{exact}}|_{max}$
$q_{3,S}/|q_{3,S_{exact}}|_{max}$
$q_{2,A}/|q_{2,A_{exact}}|_{max}$
$q_{1,A}/|q_{1,A_{exact}}|_{max}$
$T_S/|T_{S_{exact}}|_{max}$
$q_{3,A}/|q_{3,A_{exact}}|_{max}$
$q_{2,S}/|q_{2,S_{exact}}|_{max}$
$q_{1,S}/|q_{1,S_{exact}}|_{max}$

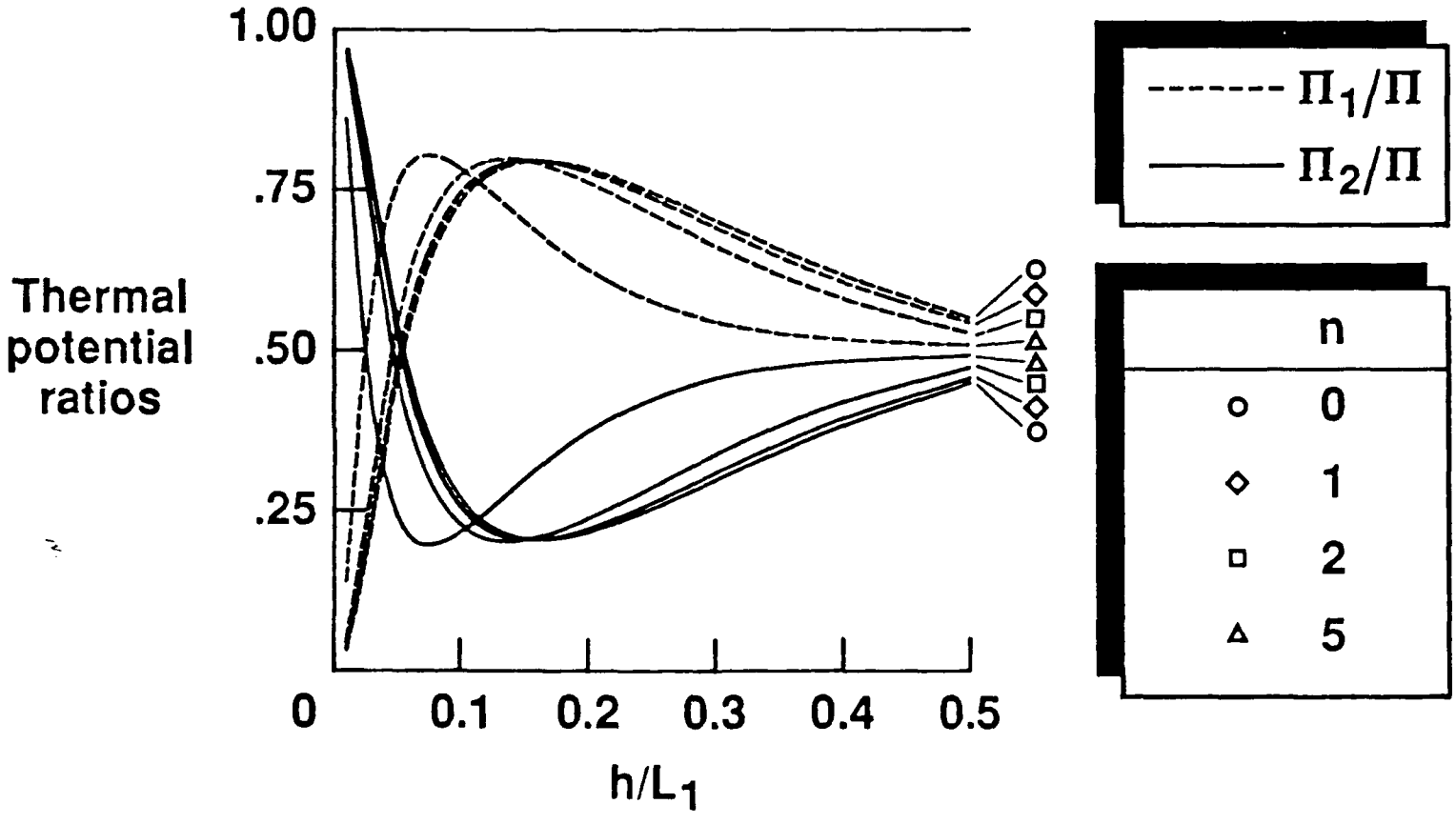
Thermal potential ratios
1.00
.75
.50
.25
0
0.1
0.2
0.3
0.4
0.5
h/L1
Π1/Π
Π2/Π
n
0
1
2
5

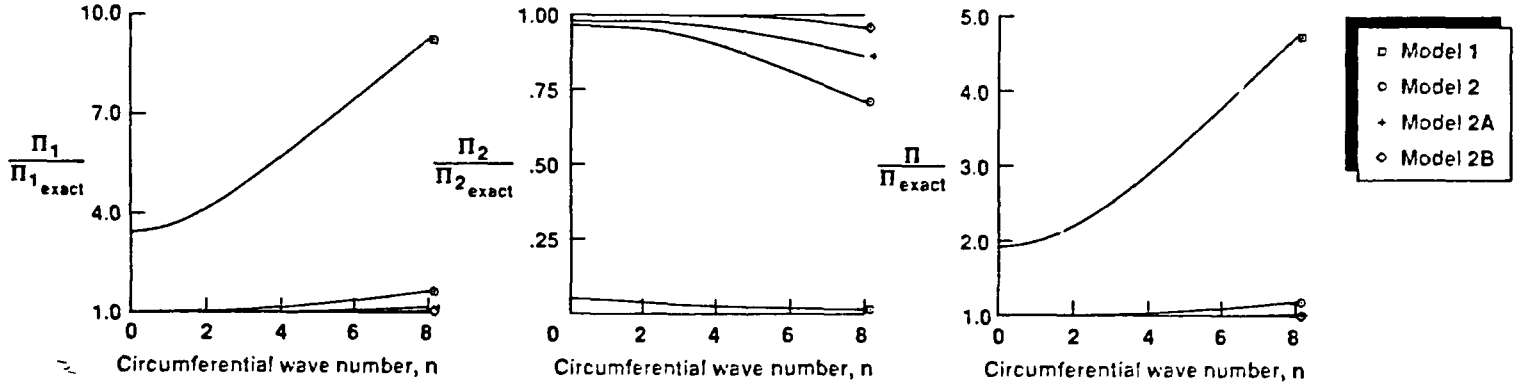
10.0
7.0
4.0
1.0
$\frac{\Pi_1}{\Pi_{1_{exact}}}$
0
2
4
6
8
Circumferential wave number, n
1.00
.75
.50
.25
$\frac{\Pi_2}{\Pi_{2_{exact}}}$
0
2
4
6
8
Circumferential wave number, n
5.0
4.0
3.0
2.0
1.0
$\frac{\Pi}{\Pi_{exact}}$
0
2
4
6
8
Circumferential wave number, n
Model 1
Model 2
Model 2A
Model 2B

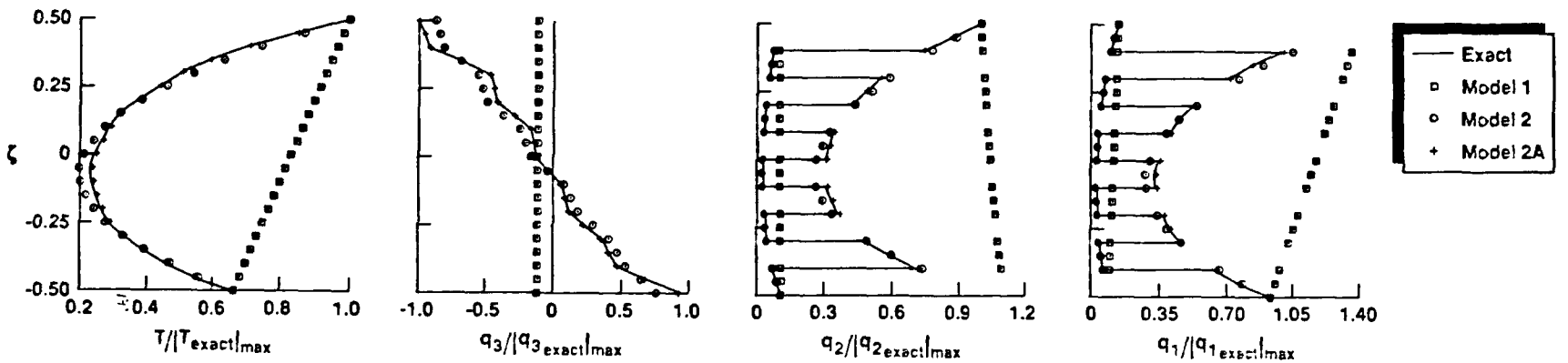
0.50
0.25
0
-0.25
-0.50
ζ
0.2
0.4
0.6
0.8
1.0
T/|T exact|max
-1.0
-0.5
0
0.5
1.0
q3/|q3 exact|max
0
0.3
0.6
0.9
1.2
q2/|q2 exact|max
0
0.35
0.70
1.05
1.40
q1/|q1 exact|max
Exact
Model 1
Model 2
Model 2A